Lecture Notes in Computational Science and Engineering

40

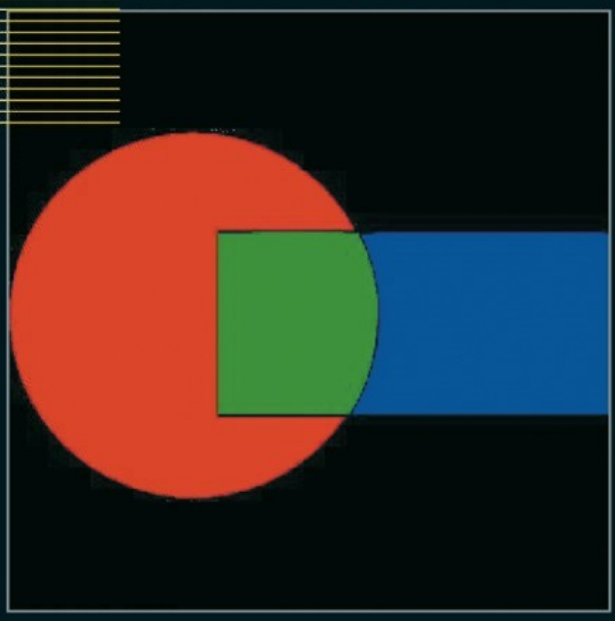

Ralf Kornhuber
Ronald Hoppe
Jacques Périaux
Olivier Pironneau
Olof Widlund
Jinchao Xu
Editors

Domain Decomposition Methods in Science and Engineering

Springer

Lecture Notes
in Computational Science
and Engineering

40

Ralf Kornhuber
Ronald Hoppe
Jacques Périaux
Olivier Pironneau
Olof Widlund
Jinchao Xu
Editors

Domain Decomposition Methods in Science and Engineering

With 184 Figures

Springer

Editors

Ralf Kornhuber

Fachbereich Mathematik und
Informatik
Freie Universität Berlin
Arnimallee 2-6
14195 Berlin, Germany
e-mail: kornhuber@math.fu-berlin.de

Ronald Hoppe

Department of Mathematics
University of Houston
Philip G. Hoffman Hall 651
77204-3008 Houston, TX, USA
e-mail: rohop@math.uh.edu

Jacques Périaux

Dassault Aviation
78 Quai Marcel Dassault
Cedex 300
92552 St. Cloud, France
e-mail:
jacques.periaux@dassault-aviation.fr

Olivier Pironneau

Laboratoire Jacques-Louis Lions
Université Paris VI
175 Rue de Chevaleret
75013 Paris, France
e-mail:
olivier.pironneau@ann.jussieu.fr

Olof Widlund

Courant Institute of Mathematical
Science
New York University
Mercer Street 251
10012 New York, USA
e-mail: widlund@cims.nyu.edu

Jinchao Xu

Department of Mathematics
Eberly College of Science
Pennsylvania Sate University
McAllister Building 218
16802 University Park, PA, USA
e-mail: xu@math.psu.edu

Library of Congress Control Number: 2004111962

Mathematics Subject Classification (2000): 65M55, 65Y05

ISSN 1439-7358
ISBN 3-540-22523-4 Springer Berlin Heidelberg New York

Springer is a part of Springer Science+Business Media
springeronline.com

Printed in Germany

Cover Design: Friedhelm Steinen-Broo, Estudio Calamar, Spain
Cover production: *design & production*, Heidelberg
Typeset by the authors using a Springer TEX macro package
Production: LE-TEX Jeloneck, Schmidt & Vöckler GbR, Leipzig

Printed on acid-free paper 46/3142/YL - 5 4 3 2 1 0

Preface

This volume contains a selection of 72 papers presented at the 15$^{\text{th}}$ International Conference on Domain Decomposition which was hosted by Freie Universität Berlin (FU) in cooperation with Zuse Institute Berlin (ZIB), Weierstrass Institute Berlin (WIAS) and the DFG Research Center 'Mathematics for Key Technologies' in Berlin, Germany, July 21 - 25, 2003. The attendance of 167 scientists from 24 countries accentuates the relevance of this series of almost annual meetings. In addition, an introductory tutorial by William D. Gropp and David E. Keyes arranged in the run up to the conference attracted 31 participants from all parts of the world, most of which were students. The conference itself included 15 plenary lectures delivered by leading experts in the field, 12 Minisymposia, 37 contributed talks and a poster session. A total of 144 presentations made this meeting one of the largest in the series of domain decomposition conferences. Since three parallel sessions were employed in order to accommodate as many presenters as possible, attendees and non-attendees alike may turn to this volume to keep up with future trends that might be guessed from the diversity of subjects.

Domain decomposition conferences have become the most important market place world wide for exchanging and discussing new ideas about the old algorithmic paradigm of 'divide and conquer'. Much of this reputation stems from the close interaction of experts in numerical analysis and practitioners from various fields of application concerning *fast and reliable iterative methods* for discretized partial differential equations: Schwarz methods and substructuring techniques form today's basis for large scale parallel computing. The unified view on the decomposition into subdomains and the decomposition into frequencies in terms of abstract Schwarz methods or subspace correction bridged the gap between domain decomposition and multigrid. Sophisticated finite element tearing and interconnecting techniques opened new perspectives (not only) in linear elasticity.

While classical domain decomposition concentrates on a given discretized PDE, coupling/decoupling techniques have meanwhile been applied successfully to derive efficient solution procedures including the *discretization* itself:

Mortar finite elements are most famous for their flexibility, e.g., with respect to non-matching grids, a property which is particularly attractive in multi-body contact. Other promising results concern the fast solution of time-dependent problems by waveform relaxations with optimized coupling conditions or by parareal algorithms.

The two latter approaches are motivated by parallel computation. On the other hand, it is the underlying physical background that motivates, e.g., the splitting of problems on an unbounded domain into a bounded and an unbounded part and gives rise to different discretizations in these subdomains together with suitable coupling conditions. Many other physical problems involve the localisation of the physics and their transient variability across the geometric domain. For the mathematical description of such heterogeneous processes it is important to understand various options of coupling subdomains in relation to the overall multi-physics problem. In this way, heterogeneous domain decomposition can be regarded as a new and promising approach to the *mathematical modeling* of complex phenomena on multiple scales.

This volume reviews recent developments in mathematical modeling, discretization, and fast and reliable solution by domain decomposition or related techniques, including implementation issues. Applications comprise biocomputing, computational mechanics, combustion, electromagnetics, electronic packaging, electrodynamics, fluid dynamics, medicine, metallurgy, microwave technology, optimal control, porous media flow, and voice generation. For the convenience of readers coming recently into the subject, a bibliography of previous proceedings is provided below, along with some major recent review articles and related special interest volumes. This list will inevitably be found embarrassingly incomplete. (No attempt has been made to supplement this list with the larger and closely related literature of multigrid and general iterative methods, except for the books by Hackbusch and Saad, which have significant domain decomposition components.)

P. Bjørstad, M. Espedal, and D. Keyes, editors. *Proc. Ninth Int. Conf. on Domain Decomposition Methods for Partial Differential Equations*, Ullensvang, 1997. Wiley, New York, 1999.

T. Chan, R. Glowinski, J. Périaux, and O. Widlund, editors. *Proc. Second Int. Symp. on Domain Decomposition Methods for Partial Differential Equations*, Los Angeles, 1988. SIAM, Philadelphia, 1989.

T. Chan, R. Glowinski, J. Périaux, and O. Widlund, editors. *Proc. Third Int. Symp. on Domain Decomposition Methods for Partial Differential Equations*, Houston, 1989. SIAM, Philadelphia, 1990.

T. Chan, T. Kako, H. Kawarada, and O. Pironneau, editors. *Proc. Twelfth Int. Conf. on Domain Decomposition Methods for Partial Differential Equations*, Chiba, 1999. DDM.org, Bergen, 2001.

T. Chan and T. Mathew. Domain decomposition algorithms. *Acta Numerica*, pages 61–143, 1994.

M. Débit, M. Garbey, R. Hoppe, D. Keyes, Y. Kuznetsov, and J. Périaux, editors. *Proc. Thirteenth Int. Conf. on Domain Decomposition Methods for Partial Differential Equations*, Lyon, 2000. CINME, Barcelona, 2002.

C. Farhat and F.-X. Roux. Implicit parallel processing in structural mechanics. *Computational Mechanics Advances*, 2:1–124, 1994.

R. Glowinski, G. Golub, G. Meurant, and J. Périaux, editors. *Proc. First Int. Symp. on Domain Decomposition Methods for Partial Differential Equations*, Paris, 1987. SIAM, Philadelphia, 1988.

R. Glowinski, Y. Kuznetsov, G. Meurant, J. Périaux, and O. Widlund, editors. *Proc. Fourth Int. Symp. on Domain Decomposition Methods for Partial Differential Equations*, Moscow, 1990. SIAM, Philadelphia, 1991.

R. Glowinski, J. Périaux, Z.-C. Shi, and O. Widlund, editors. *Proc. Eighth Int. Conf. on Domain Decomposition Methods for Partial Differential Equations*, Beijing, 1995. Wiley, Strasbourg, 1997.

W. Hackbusch. *Iterative Methods for Large Sparse Linear Systems*. Springer, Heidelberg, 1993.

I. Herrera, D. Keyes, O. Widlund, and R. Yates, editors. *Proc. Fourteenth Int. Conf. on Domain Decomposition Methods in Science and Engineering*, Cocoyoc, 2002. UNAM, Mexico City, 2003.

D. Keyes, T. Chan, G. Meurant, J. Scroggs, and R. Voigt, editors. *Proc. Fifth Int. Conf. on Domain Decomposition Methods for Partial Differential Equations*, Norfolk, 1991. SIAM, Philadelphia, 1992.

D. Keyes, Y. Saad, and D. Truhlar, editors. *Domain-based Parallelism and Problem Decomposition Methods in Science and Engineering*, 1995. SIAM, Philadelphia.

D. Keyes and J. Xu, editors. *Proc. Seventh Int. Conf. on Domain Decomposition Methods for Partial Differential Equations*, PennState, 1993. AMS, Providence, 1995.

B. Khoromskij and G. Wittum. *Numerical Solution of Elliptic Differential Equations by Reduction to the Interface*. Springer, 2004.

C.-H. Lai, P. Bjørstad, M. Cross, and O. Widlund, editors. *Proc. Eleventh Int. Conf. on Domain Decomposition Methods for Partial Differential Equations*, Greenwich, 1999. DDM.org, Bergen, 2000.

P. Le Tallec. Domain decomposition methods in computational mechanics. *Computational Mechanics Advances*, 2:121–220, 1994.

J. Mandel, C. Farhat, and X.-C. Cai, editors. *Proc. Tenth Int. Conf. on Domain Decomposition Methods for Partial Differential Equations*, Boulder, 1998. AMS, Providence, 1999.

L. Pavarino and A. Toselli. *Recent Developments in Domain Decomposition Methods*, volume 23 of *Lecture Notes in Computational Science & Engineering*. Springer, 2002.

A. Quarteroni, J. Périaux, Y. Kuznetsov, and O. Widlund, editors. *Proc. Sixth Int. Conf. on Domain Decomposition Methods for Partial Differential Equations*, Como, 1992. AMS, Providence, 1994.
A. Quarteroni and A. Valli. *Domain Decomposition Methods for Partial Differential Equations*. Oxford, 1999.
Y. Saad. *Iterative Methods for Sparse Linear Systems*. PWS, Boston, 1996.
B. Smith, P. Bjørstad, and W. Gropp. *Domain Decomposition: Parallel Multilevel Algorithms for Elliptic Partial Differential Equations*. Cambridge Univ. Press, Cambridge, 1996.
A. Toselli and O. Widlund. *Domain Decomposition Methods*. Springer, 2004.
B. Wohlmuth. *Discretization Methods and Iterative Solvers on Domain Decomposition*. Springer, 2001.
J. Xu. Iterative methods by space decomposition and subspace correction. *SIAM Review*, 34:581–613, 1991.

We also recommend the homepage for domain decomposition on the World Wide Web `www.ddm.org` maintained by Martin Gander. This site features links to past and future conferences, a growing number of conference proceedings together with updated bibliographic and personal information pertaining to domain decomposition.

We wish to thank all members of the Scientific Committee for Domain Decomposition Conferences, and in particular the chair Ronald H.W. Hoppe, for their help in setting the scientific direction of this conference. We are also grateful to the organizers of the minisymposia for shaping the profile of the scientific program and attracting high-quality presentations. The conference offered a fruitful integration of scientific excellence of speakers with a great level of interaction not only during the sessions but also along the friendly conference dinner under the 'communication tent', bringing a pleasant and relaxed atmosphere for exchanging information among attendees and lecturers. The local organization was carried out by a wonderful team of almost 50 members of FU Berlin, Zuse Institute Berlin (ZIB), and Weierstrass Institute Berlin (WIAS). We thank all members of the local organizing committee chaired by Ralf Kornhuber and, most notably, the conference manager Sabrina Nordt for perfectly taking care of all aspects of preparing and running DD15.

We gratefully acknowledge the financial and logistic support of this conference by FU Berlin, WIAS, ZIB, the German Research Foundation (DFG), and, last but not least, by the DFG Research Center 'Mathematics for Key Technologies'.

The timely production of these proceedings would not have been possible without the excellent cooperation of the authors and the referees. We would like to thank all of them for their graceful and timely response to our various demands. Special thanks are due to the technical editors Rainer Roitzsch and Uwe Pöhle for patiently eliminating all kinds of bugs from the final LaTeX

source and for presenting these proceedings on the web. Finally we wish to thank Martin Peters and Thanh-Ha Le Thi from Springer for a friendly, reliable, and efficient collaboration.

Ralf Kornhuber
Berlin, Germany

Ronald H.W. Hoppe
Augsburg, Germany and Houston, USA

Jacques Périaux
Paris, France

Olivier Pironneau
Paris, France

Olof B. Widlund
New York, USA

Jinchao Xu
PennState, USA

Contents

Part I

Invited Talks

Non-matching Grids and Lagrange Multipliers

S. Bertoluzza[1], F. Brezzi[1,2], L.D. Marini[1,2], and G. Sangalli[1]

[1] Istituto di Matematica Applicata e Tecnologie Informatiche del C.N.R., Pavia (`http://www.imati.cnr.it/{~aivlis,~brezzi,~marini,~sangalli}`)
[2] Università di Pavia, Dipartimento di Matematica

Summary. In this paper we introduce a variant of the three-field formulation where we use only two sets of variables. Considering, to fix the ideas, the homogeneous Dirichlet problem for $-\Delta u = g$ in Ω, our variables are *i)* an approximation ψ_h of u on the *skeleton* (the union of the interfaces of the sub-domains) on an independent grid (that could often be uniform), and *ii)* the approximations u_h^s of u in each sub-domain Ω^s (each on its own grid). The novelty is in the way to derive, from ψ_h, the values of each trace of u_h^s on the boundary of each Ω^s. We do it by solving an auxiliary problem on each $\partial\Omega^s$ that resembles the mortar method but is more flexible. Optimal error estimates are proved under suitable assumptions.

1 Introduction

Assume, for simplicity, that we have to solve the model problem

$$\text{find } u \in H_0^1(\Omega) \text{ such that} \qquad -\Delta u = g \text{ in } \Omega \quad \text{with } u = 0 \text{ on } \partial\Omega \tag{1}$$

on a polygonal or polyhedral domain $\Omega \subset \mathbb{R}^n$, $n = 2, 3$, where g is a given function sufficiently regular in Ω. In order to apply a Domain Decomposition technique we split Ω into sub-domains Ω^s $(s = 1, 2, ..., S)$ and we consider the *skeleton*

$$\Sigma := \cup_s \Gamma^s, \qquad \text{with} \qquad \Gamma^s \equiv \partial\Omega^s. \tag{2}$$

For the sake of simplicity we will use a three-dimensional notation, and speak therefore of *faces, edges* and *vertices*. The change of terminology in the polygonal case is obvious and left to the reader. On Σ we consider

$$\Phi := \{\varphi \in L^2(\Sigma) : \ \exists v \in H_0^1(\Omega) \text{ with } \varphi = v_{|\Sigma}\} \equiv H_0^1(\Omega)_{|\Sigma} \equiv H^{1/2}(\Sigma). \tag{3}$$

In each Ω^s we consider instead

$$V^s := \{v^s \in H^1(\Omega^s) \text{ such that } \exists v \in H_0^1(\Omega) \text{ with } v^s = v_{|\Omega^s}\}, \tag{4}$$

that can also be seen as the set of functions in $H^1(\Omega^s)$ that vanish at the intersection (if any) of Γ^s with $\partial\Omega$. In its turn, $H^1_0(\Omega)$ could be identified with a subspace of

$$V := \{u \in L^2(\Omega),\ u|_{\Omega^s} \in V^s\}, \tag{5}$$

and in particular, setting $v^s := v|_{\Omega^s}$ we can write

$$H^1_0(\Omega) \simeq \{v \in V \text{ such that } \exists \varphi \in \Phi \text{ with } v^s = \varphi \text{ on } \Gamma^s, \quad s = 1, ..., S\}. \tag{6}$$

For each s we will also introduce the trace space $\Theta^s = H^{1/2}(\Gamma^s)$, and we set $\Theta = \prod_s \Theta^s$. For $v \in V$, $\theta = (\theta^1, \ldots, \theta^s) \in \Theta$ we will write

$$v|_\Sigma = \theta \text{ to indicate that } \theta^s = v^s|_{\Gamma^s} \text{ (with } v^s = v|_{\Omega^s}), \quad s = 1, \ldots, S.$$

When discretizing the problem, we assume to be given a decomposition $\mathcal{T}^\Sigma_\delta$ of Σ and a corresponding space $\Phi_\delta \subset \Phi$ of piecewise polynomials. We also assume that in each Ω^s we are given a decomposition $\mathcal{T}^s_h \equiv \mathcal{T}^{\Omega^s}_h$ with a corresponding space $V^s_h \subset V^s$ of piecewise polynomials, and we set

$$V_h := \{v \in V \text{ such that } v|_{\Omega^s} \in V^s_h\}. \tag{7}$$

It is clear that each decomposition $\mathcal{T}^s_h$ will induce a decomposition $\mathcal{T}^{\Gamma^s}_h$ on Γ^s and a corresponding space of traces $\Theta^s_h \subset \Theta^s$. On the other hand the restriction of $\mathcal{T}^\Sigma_\delta$ to Γ^s also induces a decomposition $\mathcal{T}^{\Gamma^s}_\delta$ of Γ^s and another space of piecewise polynomials Φ^s_δ made by the restrictions of the functions in Φ_δ to Γ^s. Hence, on each Γ^s we have *two* decompositions (one coming from $\mathcal{T}^\Sigma_\delta$ and one from $\mathcal{T}^s_h$) and two spaces of piecewise polynomial functions (one from Φ_δ and one from V^s_h). Note, incidentally, that on each face f belonging to two different sub-domains we will have *three* decompositions and three spaces: one from Σ and the other two from the two sub-domains.

The first basic idea of our method is to design for every sub-domain Ω^s a linear operator $\mathcal{G}^s$ (the *generation operator*) that maps every *mother* $\varphi_\delta \in \Phi_\delta$ into an element (*daughter*) $\theta^s_h = \mathcal{G}^s(\varphi_\delta) \in \Theta^s_h$. Together with the individual $\mathcal{G}^s$ we consider a *global* operator $\mathcal{G}$ defined as

$$\mathcal{G}(\varphi_\delta) = (\theta^1_h, \ldots, \theta^S_h) \in \Theta_h \quad \text{ with } \theta^s = \mathcal{G}^s(\varphi_\delta). \tag{8}$$

The way to construct the operators $\mathcal{G}^s$ constitutes the second basic idea of this paper, and will be described in a while.

Once we have the operators $\mathcal{G}^s$ we can consider the subspace $\mathcal{S}_h$ of V_h made of *sisters* (that is, daughters of the same mother):

$$\mathcal{S}_h := \{v_h \in V_h \text{ such that } \exists \varphi_\delta \in \Phi_\delta \text{ with } v_{h|\Sigma} = \mathcal{G}(\varphi_\delta)\} \subseteq V. \tag{9}$$

We point out that in our previous definitions we consider as *daughter*, at the same time, an element θ^s_h $(= v^s_h|_{\Gamma^s})$ of Θ^s_h, and any function $v^s_h \in V^s_h$ having that same trace. It is clear, comparing (9) with (6), that $\mathcal{S}_h$ can be seen

as a nonconforming approximation of $H_0^1(\Omega)$. This allows us to consider the following discrete formulation. We set

$$a_s(u,v) := \int_{\Omega^s} \nabla u \cdot \nabla v \mathrm{d}x \qquad \text{and} \qquad a(u,v) := \sum_{s=1}^{S} a_s(u^s, v^s) \tag{10}$$

and we look for $u_h \in \mathcal{S}_h$ such that

$$a(u_h, v_h) = \int_{\Omega} g\, v_h \mathrm{d}x \quad \forall v_h \in \mathcal{S}_h. \tag{11}$$

It is clear that, under reasonable assumptions on the subspaces Φ_δ and V_h^s and on the generation operators $\mathcal{G}^s$, problem (11) will have good stability and accuracy properties.

The idea of imposing weak continuity by introducing the space Φ_δ and define a nonconforming approximation of $H_0^1(\Omega)$ by taking the subset of V_h whose elements take (in some weak sense) value $\varphi_h \in \Phi_\delta$ is one of the main ideas of the three field formulation (Brezzi and Marini [1994]). Following that approach, for each sub-domain Ω^s we could take a space M_h^s of Lagrange multipliers, and, for every $\varphi_\delta \in \Phi_\delta$, we could define $\mathcal{G}^s(\varphi_\delta) \in \Theta_h^s$ by

$$\int_{\Gamma^s} (\varphi_\delta - \mathcal{G}^s(\varphi_\delta))\mu_h^s \,\mathrm{d}x = 0 \qquad \forall \mu_h^s \in M_h^s. \tag{12}$$

In general, however, equation (12) does not define $\mathcal{G}^s(\varphi_d elta)$ uniquely, even when the spaces M_h^s and Θ_h^s satisfy the required *inf-sup* condition (see (24)). Though this is not a problem in the definition and in the analysis of the three field formulation, we would like to point out that having the trace of the elements v_h^s on Γ^s somehow uniquely determined by an element of Φ_δ has some clear advantage from the point of view of implementation. In particular it allows to use standard Dirichlet solvers (which can easily be found already implemented and whose optimization is well understood) as a brick for treating the equation in the subdomain. In order for $\mathcal{G}^s(\varphi_\delta)$ to be uniquely determined by (12) the spaces M_h^s and Θ_h^s must have the same dimension. A simple minded choice is $M_h^s \equiv \Theta_h^s$, that guarantees existence and uniqueness of the solution of (12) together with optimal stability and accuracy properties of the projector $\mathcal{G}^s$. This choice however is not the optimal one: in fact, during the estimate of the error for problem (11), there seems to be no way to get rid of a term like

$$\sum_s \int_{\Gamma^s} \frac{\partial u}{\partial \mathbf{n}_s} (\varphi_\delta - \mathcal{G}^s(\varphi_\delta)) \,\mathrm{d}x. \tag{13}$$

An obvious way to treat the term in (13) is to use the fact that $\varphi_\delta - \mathcal{G}^s(\varphi_\delta)$ is orthogonal to all elements in M_h^s, so that we can subtract from $\partial u/\partial \mathbf{n}_s$ any element of M_h^s. In particular we are interested in subtracting a suitable approximation $\mu_I^s \simeq \partial u/\partial \mathbf{n}_s$. It is then crucial to be able to find in M_h^s a μ_I^s that approximates $\partial u/\partial \mathbf{n}_s$ with the needed order. However, $\partial u/\partial \mathbf{n}_s$ is

discontinuous passing from one face to another of the same Ω^s. And if the space M_h^s is made of *continuous* functions (as it would be with the choice $M_h^s \equiv \Theta_h^s$), then the order of approximation (say, in $H^{-1/2}(\partial\Omega^s)$) cannot be better than $O(h)$ (and actually with some additional logarithmic loss, as $O(h|\lg h|)$. Hence, we do need an M_h^s made of functions that can be discontinuous when passing from one face to another of the same Ω^s. The requirement to contain a suitable amount of discontinuities and the one to have the same dimension of Θ_h^s seem very difficult to conciliate. Actually, a quite similar difficulty is met in the *mortar method*, (see e.g. Bernardi et al. [1993], Belgacem and Maday [1997], Hoppe et al. [1998], Wohlmuth [2001]), in particular in three dimensions. There, the requirement that M_h^s have the same dimension as Θ_h^s is relaxed as little as possible. The values of a "weakly continuous" function v_h^s at nodes which are interior to the faces of Γ^s on the slave sides are uniquely determined by the weak continuity equation, while the degrees of freedom corresponding to nodes on the edges of Γ^s (whose union forms the so called wirebasket) are free. We point out that the mortar method can be described in the framework given here provided we relax the assumption $\Phi_\delta \subset H^{1/2}(\Sigma)$ by allowing the functions ϕ_δ to be discontinuous across the "wirebasket": Φ_δ would correspond to the traces of v_h on the "master sides" (or "mortars") and $\mathcal{G}^s$ being defined as the identity on master sides and to one of the available mortar projections on "slave sides".

The idea, here, is to give up the equality of the dimensions but still obtain a well defined operator $\mathcal{G}^s$, by changing (12) in a slightly more complicated formulation, involving an additional Lagrange multiplier. Let us see the main features of this path.

We choose first a space M_h^s having in mind the fact that we must be able to use it for approximating $\partial u/\partial \mathbf{n}_s$ with the right order. We also need its dimension to be smaller than (or equal to) that of Θ_h^s. Then we change (12) in the following way. For every $\varphi_\delta \in \Phi_\delta$ we look for *a pair* $(\widetilde{\theta_h^s}, \widetilde{\mu_h^s})$ in $\Theta_h^s \times M_h^s$ such that

$$\int_{\Gamma^s} (\varphi_\delta - \widetilde{\theta_h^s})\, \mu_h^s \, \mathrm{d}x = 0 \qquad \forall \mu_h^s \in M_h^s \tag{14}$$

and

$$\sum_{T \in \mathcal{T}_h^{\Gamma^s}} \int_T h_T^{-1} (\varphi_\delta - \widetilde{\theta_h^s})\, \theta_h^s \, \mathrm{d}x + \int_{\Gamma^s} \widetilde{\mu_h^s}\, \theta_h^s \, \mathrm{d}x = 0 \qquad \forall \theta_h^s \in \Theta_h^s. \tag{15}$$

Then we set

$$\mathcal{G}^s(\varphi_\delta) := \widetilde{\theta_h^s}. \tag{16}$$

It is clear that in (14)-(15) the number of equations will always be equal to the number of unknowns. It is also clear that if (by shear luck) we have $\varphi_\delta|_{\Gamma^s} \in \Theta_h^s$ then $\mathcal{G}^s(\varphi_\delta) = \varphi_\delta|_{\Gamma^s}$ (and $\widetilde{\mu_h^s} = 0$). This will, in the end, provide for the new approach (14)-(16) an optimal order of accuracy (as we had for the previous simple-minded (12)). It is, finally, also obvious that some sort of

inf-sup condition will be needed in order to ensure existence and uniqueness of the solution of (14)-(15), unless some suitable additional stabilization is introduced. However, as we shall see, the possibility of escaping the cage of the equal dimensionality of M_h^s and Θ_h^s opens a whole lot of interesting possibilities.

In this paper we will follow the path indicated above. In the next section we will make precise all the necessary assumptions, and in Section 3 we will derive abstract error bounds for problem (11) when the operators $\mathcal{G}^s$ are constructed as in (14)-(16). In Section 4 we will present some possible choices for the finite element spaces and discuss their stability and accuracy properties. In particular we will show that the simple choice of using totally discontinuous functions for M_h^s, stabilizing the problem with suitable *boundary bubbles*, leads to a problem with optimal convergence properties and, at the same time, a very simple implementation. This is reminiscent of what has been done for instance in Baiocchi et al. [1992], Brezzi et al. [1997], Buffa [2002], and Brezzi and Marini [2000], but simpler and more effective. Finally, in the last section we briefly discuss some possible variants/extensions, in particular regarding the possibility of using discontinuous mothers.

2 Assumptions on the decomposition and on the discretizations

We consider now the assumptions to be made on the decomposition and on the discretizations.

Assumptions on Ω and on the domain decomposition

We assume that Ω is an open polyhedron, that each Ω^s, for $s = 1, ..., S$, is also an open polyhedron, that the intersection of two different Ω^s is empty, and that the union of the closures of all Ω^s is the closure of Ω. As in (2) the *skeleton* Σ will be the union of the boundaries $\partial\Omega^s$. We do not assume that this decomposition is *compatible*. This means that we do not assume that the intersection of the closure of two different Ω^s is either a common face, or a common edge, or a common vertex. For simplicity we assume however that the number S of subdomains is fixed once and for all, and we do not keep track of the dependency of the various constants on S.

Assumptions on the decomposition $\mathcal{T}_\delta^\Sigma$

We assume that we are given a sequence $\{\mathcal{T}_\delta^\Sigma\}_\delta$ of decompositions of Σ. Each decomposition $\mathcal{T}_\delta^\Sigma$ is made of open triangles, in such a way that the intersection of two different triangles is empty, and the union of the closures of all triangles is Σ. We assume *compatibility*, that is we assume that the

intersection of the closures of two different triangles is either empty, a common edge or a common vertex. We also assume, as usual, *shape regularity*, for instance by assuming that the ratio between the diameter of each triangle and the radius of its biggest inscribed circle is $\leq \kappa_0$, with κ_0 independent of δ. Finally we assume *quasi-uniformity*: there exists a constant q, independent of δ such that, if δ_T^{min} and δ_T^{max} are the minimum and the maximum diameters (respectively) of the triangles in $\mathcal{T}_\delta^\Sigma$, then $\delta_T^{min} \geq q\, \delta_T^{max}$.

Assumptions on the decompositions $\mathcal{T}_h^s$ (and $\mathcal{T}_h^{\Gamma^s}$)

We assume that we are given, for each $s = 1, ..., S$, a sequence $\{\mathcal{T}_h^s\}_h$ of decompositions of Ω^s. Each decomposition is made of open tetrahedra in such a way that the intersection of two different tetrahedra is empty, and the union of the closures of all tetrahedra is Ω^s. We also assume *compatibility*: the intersection of the closures of two different tetrahedra is either empty, a common face, a common edge, or a common vertex. Finally we assume *shape regularity*, for instance by assuming that the ratio between the diameter of each tetrahedron and the radius of its biggest inscribed sphere is $\leq \kappa_1$, with κ_1 independent of h. We point out that we do not assume quasi-uniformity for the meshes $\mathcal{T}_h^s$. We recall that the triangulation $\mathcal{T}_h^{\Gamma^s}$ is the restriction on Γ^s of $\mathcal{T}_h^s$.

Assumptions on the discretizations Φ_δ, V_h^s, and M_h^s

We assume that for each δ and for each $T \in \mathcal{T}_\delta^\Sigma$ we are given a space of polynomials $\mathcal{P}_T$. The space Φ_δ will then be defined as

$$\Phi_\delta := \{\varphi \in \Phi \text{ such that } \varphi_{|T} \in \mathcal{P}_T, \quad T \in \mathcal{T}_\delta^\Sigma\}, \tag{17}$$

where Φ is always given by (3). Similarly we assume that for each s, for each h, and for each $K \in \mathcal{T}_h^s$ we are given a space of polynomials $\mathcal{P}_K$. The space V_h^s will then be defined as

$$V_h^s := \{v^s \in V^s \text{ such that } v^s_{|K} \in \mathcal{P}_K, \quad K \in \mathcal{T}_h^s\}, \tag{18}$$

where V^s is still given by (4).

The corresponding restrictions of the above spaces to each Γ^s are defined as in the previous section, namely

$$\Phi_\delta^s := (\Phi_\delta)_{|\Gamma^s} \qquad \text{and} \qquad \Theta_h^s := (V_h^s)_{|\Gamma^s}, \quad s = 1, ..., S. \tag{19}$$

We assume that there exist bounded lifting operators from Θ_h^s to V_h^s. More precisely, for all $s = 1, \ldots, S$, for all $\theta_h^s \in \Theta_h^s$ there exists $w_h^s \in V_h^s$ such that

$$w_h^s|_{\Gamma^s} = \theta_h^s \qquad \text{and} \qquad \|w_h^s\|_{1,\Omega^s} \leq C\|\theta_h^s\|_{H^{1/2}(\Gamma^s)}. \tag{20}$$

Finally we assume that for each s, for each h, and for each $T \in \mathcal{T}_h^{\Gamma^s}$ we are given a space of polynomials $\mathcal{Q}_T$. The space M_h^s will then be defined as

$$M_h^s := \{\mu \in L^2(\Gamma^s) \text{ such that } \mu_{|T} \in \mathcal{Q}_T, \quad T \in \mathcal{T}_h^{\Gamma^s}\}. \tag{21}$$

If we like, we can also add some continuity requirements to (21). In view of the discussion of the previous section, however, it would be unwise to force continuity in the passage from one face to another. In order for the bilinear form a to ve coercive in a suitable space, we make the following minimal assumption on M_h^s:

$$\text{for every } \Omega^s \text{ the space } M_h^s \text{ contains the constants on } \Gamma^s. \tag{22}$$

Moreover, for simplicity, we assume that there exists an integer number κ such that all the spaces $\mathcal{P}_T$, $\mathcal{P}_K$, and $\mathcal{Q}_T$ verify

$$\mathcal{P}_T \subseteq \mathbb{P}_\kappa(T), \qquad \mathcal{P}_K \subseteq \mathbb{P}_\kappa(K), \qquad \mathcal{Q}_T \subseteq \mathbb{P}_\kappa(T),$$

where $\mathbb{P}_\kappa(\omega)$ is the space of polynomials of degree $\leq \kappa$ on ω. Using the notation of Brezzi and Fortin [1991a] for the usual Lagrange finite element spaces we can then write

$$V_h^s \subseteq \mathcal{L}^1_\kappa(\mathcal{T}_h^s), \quad \Theta_h^s \subseteq \mathcal{L}^1_\kappa(\mathcal{T}_h^{\Gamma^s}), \quad M_h^s \subseteq \mathcal{L}^0_\kappa(\mathcal{T}_h^{\Gamma^s}), \quad \Phi_\delta \subseteq \mathcal{L}^1_\kappa(\mathcal{T}_\delta^\Sigma).$$

The operators $\mathcal{G}^s$ and the compatibility assumptions among the discretizations

Having defined the spaces Θ_h^s and M_h^s we can now consider the operators $\mathcal{G}^s$ (that will always be given by (14)-(16)) together with the global operator $\mathcal{G}$ (still given by (8)). Once we have the operators $\mathcal{G}^s$ and $\mathcal{G}$, we can define the space of sisters $\mathcal{S}_h$, always as in (9). In $\mathcal{S}_h$ we define:

$$|\!|\!| v_h |\!|\!|^2 := \sum_{s=1}^{S} \|\nabla v_h^s\|^2_{0,\Omega^s} \tag{23}$$

We can now turn to the more important assumptions, that will require some compatibility conditions among the spaces Φ_δ^s, Θ_h^s and M_h^s.

Our first assumption will deal with the well-posedness of the problem (14)-(16). As this is a problem in classical mixed form, we have no real escape but assuming an *inf-sup* condition on the spaces Θ_h^s and M_h^s:

$\exists \beta > 0$ such that $\forall s = 1, ..., S$ and $\forall h > 0$

$$\inf_{\mu_h^s \in M_h^s \setminus \{0\}} \sup_{\theta_h^s \in \Theta_h^s \setminus \{0\}} \frac{\int_{\Gamma^s} \theta_h^s \, \mu_h^s \, \mathrm{d}x}{\|\theta_h^s\|_{h,\frac{1}{2},\Gamma^s} \; \|\mu_h^s\|_{h,-\frac{1}{2},\Gamma^s}} > \beta, \tag{24}$$

were the norms in the denominator of (24) are defined, for any real r, as

$$\|\theta_h^s\|^2_{h,r,\Gamma^s} := \sum_{T\in\mathcal{T}_h^{\Gamma^s}} h_T^{-2r}\|\theta_h^s\|^2_{0,T} \tag{25}$$

and h_T is the diameter of T. Condition (24) will be, in a sense, the only nontrivial assumption that we have to take into account in the definition of our spaces V_h^s and M_h^s. However, in the next section, we are going to see some families of elements where (24) can be checked rather easily.

Our last assumption will deal with the *bound on the mother*. We point out that, so far, we did not assume that an element of the space of sisters $\mathcal{S}_h$ had a unique mother. Indeed, we do not need it. Strictly speaking, we only need that

$$\exists\gamma>0 \text{ such that: } \forall v_h\in\mathcal{S}_h, \exists\varphi_\delta\in\Phi_\delta \text{ with } \mathcal{G}(\varphi_\delta)=v_{h|\Sigma} \text{ and}$$

$$\|\varphi\|^2_\Phi := \sum_{s=1}^{S}|\varphi_\delta|^2_{H^{1/2}(\Gamma^s)} \le \gamma^2|\!|\!|v_h|\!|\!|^2. \tag{26}$$

We point out that $\|\cdot\|_\Phi$ is indeed a norm on Φ, since the elements of Φ vanish on $\partial\Omega$ (see Bertoluzza [2003]). One of the consequences of (26) is that the seminorm $|\!|\!|\cdot|\!|\!|$ is indeed a norm. In fact, given $v_h\in\mathcal{S}_h$ and letting $\varphi\in\Phi_\delta$ given by (26), provided (22) holds, it can be shown (see Bertoluzza [2003]) that

$$\|v_h\|_{0,\Omega} \le C(|\!|\!|v_h|\!|\!| + \|\varphi\|_\Phi) \le C|\!|\!|v_h|\!|\!|. \tag{27}$$

We shall discuss in the following sections whether and when this assumption is satisfied. We anticipate however that this will be another easy condition, that could be roughly summarized by: on each face f of each $\partial\Omega^s$ the mesh $\mathcal{T}_\delta^{\Gamma^s}$ (induced by $\mathcal{T}_\delta^\Sigma$) is coarser than the two meshes $\mathcal{T}_h^{\Gamma^s}$ (induced by the two $\mathcal{T}_h^s$ relative to the sub-domains having f in common).

3 Basic Error Estimates

We are now ready to analyze the problem (11) and derive abstract error estimates for it.

We start by looking in more detail to the operator $\mathcal{G}^s$. Thanks to the classical theory of mixed finite element (see Brezzi and Fortin [1991b]) we can prove the following Lemma.

Lemma 1. *Assume that the inf-sup condition* (24) *is satisfied, and let* $\varphi\in L^2(\Sigma)$*; then for every* $s=1,...,S$

$$\|\mathcal{G}^s(\varphi)\|_{h,\frac12,\Gamma^s} \le C\|\varphi\|_{h,\frac12,\Gamma^s}. \tag{28}$$

We point out that the norm $\|\cdot\|_{h,\frac12,\Gamma^s}$, induced by the bilinear form $(u,v)\to\sum_{T\in\mathcal{T}_h^{\Gamma^s}}\int_T h_T^{-1}u\,v\,\mathrm{d}x$ plays the role of a discrete $H^{1/2}(\Gamma^s)$ norm. Indeed we have the following lemma.

Lemma 2. *The following inverse inequality holds: for all* $\theta_h^s \in \Theta_h^s$

$$\|\theta_h^s\|_{H^{1/2}(\Gamma^s)} \leq C\|\theta_h^s\|_{h,\frac{1}{2},\Gamma^s} \tag{29}$$

Proof. We shall actually prove that (29) holds for all $\theta_h^s \in \mathcal{L}_\kappa^1(\mathcal{T}_h^{\Gamma^s})$. It is well known that a function in $\mathcal{L}_\kappa^1(\mathcal{T}_h^s)$ is uniquely identified by its values at a set $\{x_i\}_i$ of nodes corresponding to the canonical Lagrange basis. Let $\theta_h^s \in \mathcal{L}_\kappa^1(\mathcal{T}_h^{\Gamma^s})$ and let $w_h \in \mathcal{L}_\kappa^1(\mathcal{T}_h^s)$ be its finite element lifting, i.e., the function verifying $w_h^s(x_i) = \theta_h^s(x_i)$ at all nodes on Γ^s and $w_h^s(x_i) = 0$ at all other nodes. Clearly, $\|\theta_h^s\|_{H^{1/2}(\Gamma^s)} \leq C\|w_h^s\|_{H^1(\Omega^s)}$. Let us then bound the $H^1(\Omega^s)$ norm of w_h^s. By definition w_h^s is different from 0 only on those tetrahedra $T \in \mathcal{T}_h^s$ which are adjacent to the boundary. Let K be one of such tetrahedra and let $T_i \in \mathcal{T}_h^{\Gamma^s}$, $i = 1, \ldots, m$ be the triangles that share one or more nodes with K. Thanks to usual arguments, we can write:

$$\|w_h^s\|_{H^1(K)}^2 \leq Ch_K^{-1}\|w_h^s\|_{L^2(\partial K)}^2 \leq C\sum_{i=1}^m h_{T_i}^{-1}\|w_h^s\|_{L^2(T_i)}^2.$$

Adding with respect to all elements K adjacent to Γ^s, we obtain that

$$\|w_h^s\|_{H^1(\Omega^s)} \leq C\|\theta_h^s\|_{h,\frac{1}{2},\Gamma^s},$$

which implies (29).

Remark 1. Note that if we had assumed the quasi-uniformity of the triangulation $\mathcal{T}_h^{\Gamma^s}$, then (29) could easily be obtained by space interpolation, using the standard inverse inequality between the H^1 and the L^2 norms. This is however not the case, and in the above proof we only made use of the regularity of the mesh.

Lemma 2 trivially implies the continuity of $\mathcal{G}^s$ from $L^2(\Gamma^s)$ (endowed with the norm $\|\cdot\|_{h,\frac{1}{2},\Gamma^s}$), to $H^{1/2}(\Gamma^s)$. However a stronger result holds, stated in the following theorem

Theorem 1. $\mathcal{G}^s(\cdot)$ *is continuous from* $H^{1/2}(\Gamma^s)$ *to* $H^{1/2}(\Gamma^s)$*:*

$$\|\mathcal{G}^s(\varphi)\|_{H^{1/2}(\Gamma^s)} \leq C\|\varphi\|_{H^{1/2}(\Gamma^s)}. \tag{30}$$

Proof. First, we introduce the Clément interpolant $\theta_I^s \in \Theta_h^s$ of $\theta^s = \varphi|_{\Gamma^s}$, which gives (see Clément [1975])

$$\begin{aligned} \|\theta_I^s\|_{H^{1/2}(\Gamma^s)} &\leq C\|\theta^s\|_{H^{1/2}(\Gamma^s)} \\ \|\theta^s - \theta_I^s\|_{h,\frac{1}{2},\Gamma^s} &\leq C\|\theta^s\|_{H^{1/2}(\Gamma^s)}. \end{aligned} \tag{31}$$

Since $\mathcal{G}^s(\cdot)$ is linear and using the triangle inequality, we have

$$\|\mathcal{G}^s(\theta^s)\|_{H^{1/2}(\Gamma^s)} \leq \|\mathcal{G}^s(\theta^s - \theta_I^s)\|_{H^{1/2}(\Gamma^s)} + \|\mathcal{G}^s(\theta_I^s)\|_{H^{1/2}(\Gamma^s)} = I + II.$$

Making use of Lemma 2, Lemma 1 and (31), we get

$$\begin{aligned} I = \|\mathcal{G}^s(\theta - \theta_I^s)\|_{H^{1/2}(\Gamma^s)} &\leq C\|\mathcal{G}^s(\theta - \theta_I^s)\|_{h,\frac{1}{2},\Gamma^s} \\ &\leq C\|\theta - \theta_I^s\|_{h,\frac{1}{2},\Gamma^s} \\ &\leq C\|\theta\|_{H^{1/2}(\Gamma^s)}. \end{aligned}$$

Moreover, since $\mathcal{G}^s(\theta_I^s) = \theta_I^s$ and using (31), we have

$$II = \|\mathcal{G}^s(\theta_I^s)\|_{H^{1/2}(\Gamma^s)} \leq C\|\theta\|_{H^{1/2}(\Gamma^s)},$$

giving (30).

We can now prove our error estimate. From the definition (10) and assumption (27) we easily get that problem (11) has a unique solution. Let now ψ_I be an interpolant of the exact solution u in Φ_δ. For every Ω^s $(s = 1, ..., S)$ let $u_I^s \in V_h^s$ be defined as the unique solution of

$$\begin{cases} u_I^s = \mathcal{G}^s(\psi_I) \text{ on } \Gamma^s \\ a_s\,(u_I^s, v_h^s) = \int_{\Omega^s} g\, v_h^s \,\mathrm{d}x \qquad \forall v_h^s \in V_h^s \cap H_0^1(\Omega^s). \end{cases} \tag{32}$$

It is obvious that (32) has a unique solution. Let u_I be equal to u_I^s in each Ω^s $(s = 1, ..., S)$. It is clear that $u_I \in \mathcal{S}_h$. We now set $e_h := u_I - u_h \in \mathcal{S}_h$. Using the the definition (10) and adding and subtracting u we have:

$$|\!|\!| e_h |\!|\!|^2 = a\,(e_h, e_h) = a\,(u_I - u, e_h) + a\,(u - u_h, e_h) =: I + II. \tag{33}$$

Using (11) and integrating $a\,(u, e_h)$ by parts in each Ω^s we obtain

$$\begin{aligned} II = a\,(u - u_h, e_h) &= -\sum_{s=1}^{S} \int_{\Omega^s} g\, e_h^s \,\mathrm{d}x + \sum_{s=1}^{S} \int_{\Gamma^s} \frac{\partial u}{\partial \mathbf{n}^s} e_h^s \,\mathrm{d}x - \sum_{s=1}^{S} \int_{\Omega^s} g\, e_h^s \,\mathrm{d}x \\ &= \sum_{s=1}^{S} \int_{\Gamma^s} \frac{\partial u}{\partial \mathbf{n}^s} e_h^s \,\mathrm{d}x. \end{aligned} \tag{34}$$

As $e_h \in \mathcal{S}_h$, and using assumption (26) there will be a mother $\eta_\delta \in \Phi_\delta$ with $\|\eta_\delta\|_\Phi \leq C|\!|\!| e_h |\!|\!|$, such that $\mathcal{G}(\eta_\delta) = e_h|_\Sigma$. Hence the continuity of $\partial u/\partial \mathbf{n}$, and the fact that η_δ is single-valued on the skeleton Σ yield

$$II = \sum_{s=1}^{S} \int_{\Gamma^s} \frac{\partial u}{\partial \mathbf{n}^s} (e_h^s - \eta_\delta) \,\mathrm{d}x = \sum_{s=1}^{S} \int_{\Gamma^s} \frac{\partial u}{\partial \mathbf{n}^s} (\mathcal{G}^s(\eta_\delta) - \eta_\delta) \,\mathrm{d}x. \tag{35}$$

We can now use the definition of $\mathcal{G}^s$ (see (15)) and subtract from $\partial u/\partial \mathbf{n}$ its best approximation μ_I^s, thus obtaining

$$II = \sum_{s=1}^{S} \int_{\Gamma^s} \Big(\frac{\partial u}{\partial \mathbf{n}^s} - \mu_I^s\Big)(\mathcal{G}^s(\eta_\delta) - \eta_\delta) \,\mathrm{d}x. \tag{36}$$

We remember now that $\mathcal{G}^s(\eta_\delta) = e_h^s$ on Γ^s for all s. We also point out that (thanks to (22)) we can assume that the mean value of $\partial u/\partial \mathbf{n}^s - \mu_I^s$ on each Γ^s is zero, so that we can use the $H^{1/2}$-seminorm of e^s and η_δ instead of the norm in the estimate. Then we use Cauchy-Schwarz inequality, we use (26) for η_δ, and (27) standard trace inequality in each Ω^s for e^s to obtain

$$II \leq \sum_{s=1}^{S} \|\frac{\partial u}{\partial \mathbf{n}^s} - \mu_I^s\|_{H^{-1/2}(\Gamma^s)} \left(|e^s|_{H^{1/2}(\Gamma^s)} + |\eta_\delta|_{H^{1/2}(\Gamma^s)} \right)$$
$$\leq \Big(\sum_{s=1}^{S} \|\frac{\partial u}{\partial \mathbf{n}^s} - \mu_I^s\|^2_{H^{-1/2}(\Gamma^s)} \Big)^{1/2} |||e_h|||. \quad (37)$$

It remains to estimate I. After the obvious

$$I = a\,(u_I - u, e_h) \leq |||u_I - u|||\,|||e_h||| \quad (38)$$

we have to estimate $|||u - u_I|||$. Using the definition (32) of u_I^s we can apply the usual theory for estimating the error for each Dirichlet problem in Ω^s. Thanks to (20) we have first

$$\|u - u_I^s\|_{1,\Omega^s} \leq C \left(\inf_{v_h^s \in V_h^s} \|u - v_h^s\|_{1,\Omega^s} + \|u - u_I^s\|_{H^{1/2}(\Gamma^s)} \right). \quad (39)$$

It is then clear that the crucial step is to estimate $\|u - u_I^s\|_{H^{1/2}(\Gamma^s)}$, for each s.

To this aim let us introduce an interpolant $\chi_I^s \in \Theta_h^s$ of $u|_{\Gamma^s}$. We can write

$$\|u - u_I^s\|_{H^{1/2}(\Gamma^s)} \equiv \|u - \mathcal{G}^s(\psi_I)\|_{H^{1/2}(\Gamma^s)}$$
$$\leq \|u - \chi_I^s\|_{H^{1/2}(\Gamma^s)} + \|\chi_I^s - \mathcal{G}^s(u)\|_{H^{1/2}(\Gamma^s)} \quad (40)$$
$$+ \|\mathcal{G}^s(u) - \mathcal{G}^s(\psi_I)\|_{H^{1/2}(\Gamma^s)} \quad (41)$$

Since $\chi_I^s = \mathcal{G}^s(\chi_I^s)$ and using Theorem 1, we easily get $\|\chi_I^s - \mathcal{G}^s(u)\|_{H^{1/2}(\Gamma^s)} = \|\mathcal{G}^s(\chi_I^s - u)\|_{H^{1/2}(\Gamma^s)} \leq C\|u - \chi_I^s\|_{H^{1/2}(\Gamma^s)}$. By a similar argument we obtain $\|\mathcal{G}^s(u - \psi_I)\|_{H^{1/2}(\Gamma^s)} \leq \|u - \psi_I\|_{H^{1/2}(\Gamma^s)}$.

We can then collect (33)-(38) and (39)–(41) in the following theorem.

Theorem 2. *Assume that the assumptions of Section 2 on the decomposition and on the discretizations are satisfied. Assume that the operators $\mathcal{G}^s$ are constructed as in* (14)-(16)*. Let u be the exact solution of* (1) *and u_h be the solution of* (11)*. Then we have*

$$|||u - u_h|||^2 \leq C \sum_{s=1}^{S} \Big(\inf_{v_h^s \in V_h^s} \|u - v_h^s\|^2_{1,\Omega^s} + \inf_{\mu_h^s \in M_h^s} \|\frac{\partial u}{\partial \mathbf{n}^s} - \mu_h^s\|^2_{H^{-1/2}(\Gamma^s)} \Big)$$
$$+ \inf_{\varphi_\delta \in \Phi_\delta} \|u - \varphi_\delta\|^2_{H^{1/2}(\Sigma)}. \quad (42)$$

4 Examples and Remarks

In this section we want to show an example of finite element discretizations that satisfy the abstract assumptions of Section 2, and derive the corresponding error bounds in terms of suitable powers of h.

We do not discuss the assumptions on the decomposition of Ω into the Ω^s. We just remark once more that it does not need to be *compatible*: for instance, the intersection of the closures of two different Ω^s can be a face of one of them and only a piece of a face of the other.

We discuss instead the choice of the finite element spaces Φ_δ, V_h^s, and M_h^s.

Assume that we are given an integer number $k \geq 1$.

For every T in the triangulation $\mathcal{T}_\delta^\Sigma$ of the skeleton Σ we choose $\mathcal{P}_T := \mathbb{P}_k(T)$, the space of polynomials of degree $\leq k$ on T. The space Φ_δ, according to (17), becomes then

$$\Phi_\delta := \{\varphi \in \Phi \text{ such that } \varphi_{|T} \in \mathbb{P}_k(T), \quad T \in \mathcal{T}_\delta^\Sigma\} = \mathcal{L}_k^1(\mathcal{T}_\delta^\Sigma) \cap \Phi \tag{43}$$

(we recall that the elements of Φ have to vanish on $\partial\Omega$ so we need to take the intersection of $\mathcal{L}_k^1(\mathcal{T}_\delta^\Sigma)$ with Φ in order to properly define Φ_δ). For each s and for every T in the triangulation $\mathcal{T}_h^{\Gamma^s}$ of Γ^s we take instead as $\mathcal{Q}_T$ the space $\mathcal{Q}_T := \mathbb{P}_{k-1}(T)$. According to (21) the space M_h^s becomes then

$$M_h^s := \{\mu \in L^2(\Gamma^s) : \ \mu_{|T} \in \mathbb{P}_{k-1}(T), \quad T \in \mathcal{T}_h^{\Gamma^s}\} = \mathcal{L}_k^0(\mathcal{T}_h^{\Gamma^s}). \tag{44}$$

We point out that Φ_δ is made of continuous functions, while M_h^s is made of functions that are, a priori, totally discontinuous from one element to another.

The choice of each V_h^s will be slightly more elaborate. For each tetrahedron $K \in \mathcal{T}_h^s$ with no faces belonging to Γ^s we take $\mathcal{P}_K := \mathbb{P}_k$. If instead K has a face f on Γ^s we consider the cubic function b_f on K that vanishes on the three remaining internal faces of K, and we augment the space $\mathbb{P}_k$ with the space B_{k+2}^f obtained multiplying b_f times the functions in $\mathcal{Q}_f \equiv \mathbb{P}_{k-1}(f)$ (that is the space of polynomials of degree $\leq k-1$ on f: remember that the face f will be one of the triangles $T \in \mathcal{T}_h^{\Gamma^s}$). If K has another face on Γ^s we repeat the operation, augmenting further the space $\mathbb{P}_k$. In summary

$$\mathcal{P}_K := \mathbb{P}_k(K) + \{\bigoplus_{f \subset \Gamma^s} B_{k+2}^f\} \equiv \mathbb{P}_k + \{\bigoplus_{f \subset \Gamma^s} b_f \mathbb{P}_{k-1}(f)\}. \tag{45}$$

We note that $\bigoplus b_f \mathbb{P}_{k-1}(f)$ is a direct sum, but its sum with $\mathbb{P}_k(K)$ is not direct whenever $k \geq 3$. This however will not be a problem for the following developments.

We can now discuss the various abstract assumptions that have been made in Section 2. To start with, condition (22) is obviously satisfied. Similarly, (20) holds as shown for instance in Bernardi et al. [to appear]. We consider then the *inf-sup* condition (24).

Lemma 3. *Let M_h^s and Θ_h^s be constructed as in* (44) *and in* (19) *with* (45)*, respectively. Then the inf-sup condition* (24) *holds true.*

Proof. For every $\mu_h^s \in M_h^s$ we construct $v_h^s \in V_h^s$ as

$$v_h^s = \sum_{T \in \mathcal{T}_h^{\Gamma^s}} h_T \, b_T \, \mu_h^s \tag{46}$$

where as before b_T is the cubic function on K (the tetrahedron having T as one of its faces) vanishing on the other three faces of K and having mean value 1 on T. It is not too difficult to check that

$$\|\mu_h^s\|_{h,-\frac{1}{2},\Gamma^s} \, \|v_h^s\|_{h,\frac{1}{2},\Gamma^s} \leq C \int_{\mathcal{T}_h^{\Gamma^s}} v_h^s \mu_h^s \tag{47}$$

that is precisely the *inf-sup* condition (24) that we need.

We consider now the other *inf-sup* that is involved in the present scheme (although we did not write it as an *inf-sup*), that is the bound on the mother (26). By applying the technique of Babuska [1973] it is not difficult to realize that if $\mathcal{T}_\delta^\Sigma$ is "coarse enough" on each face, compared with the meshes of the two sub-domains having that face in common, then

$$\inf_{\varphi_\delta \in \mathcal{L}_k^1(\mathcal{T}_\delta^{\Gamma^s}) \setminus \{0\}} \quad \sup_{\mu_h^s \in M_h^s \setminus \{0\}} \frac{\int_{\Gamma^s} \varphi_\delta \, \mu_h^s \, \mathrm{d}x}{\|\mu_h^s\|_{H^{-1/2}(\Gamma^s)} \, \|\varphi_\delta\|_{H^{1/2}(\Gamma^s)}} > \gamma_0. \tag{48}$$

It is now easy to see that (48) implies (26): let $v_h^s \in \mathcal{S}_h$, then, by definition, there exists $\varphi_\delta \in \Phi_\delta$ such that $v_h^s|_\Sigma = \varphi_\delta$. Letting $\breve{\varphi}^s = (1/|\Gamma^s|) \int_{\Gamma^s} \varphi_\delta \mathrm{d}x$ we have that $\varphi_\delta - \breve{\varphi}^s \in \mathcal{L}_k^1(\mathcal{T}_\delta^{\Gamma^s})$. Let now $\mu_h^* \in M_h^s$ be the element that realizes the supremum in (48) for such an element of $\mathcal{L}_k^1(\mathcal{T}_\delta^{\Gamma^s})$. Using (48), and then (14), we obtain

$$\gamma_0 \|\mu_h^*\|_{H^{-1/2}(\Gamma^s)} \, \|\varphi_\delta - \breve{\varphi}^s\|_{H^{1/2}(\Gamma^s)} \leq \int_{\Gamma^s} \mu_h^* \, (\varphi_\delta - \breve{\varphi}^s) \, \mathrm{d}x \tag{49}$$

$$= \int_{\Gamma^s} \mu_h^* \, \mathcal{G}^s(\varphi_\delta - \breve{\varphi}^s) \, \mathrm{d}x. \tag{50}$$

Now, since $\varphi_\delta - \breve{\varphi}^s$ has zero mean value on Γ^s, the same is true for $\mathcal{G}^s(\varphi_\delta - \breve{\varphi}^s)$ (see (14) and (22)). Then, denoting by $\breve{v}^s = (1/|\Gamma^s|) \int_{\Gamma^s} v_h^s \mathrm{d}x$ the average of v_h^s on Γ^s, we have

$$\begin{aligned} \int_{\Gamma^s} \mu_h^* \, \mathcal{G}^s(\varphi_\delta - \breve{\varphi}^s) \, \mathrm{d}x &= \int_{\Gamma^s} \mu_h^* \, (v_h^s - \breve{v}^s) \, \mathrm{d}x \\ &\leq \|\mu_h^*\|_{H^{-1/2}(\Gamma^s)} \, |v_h^s|_{H^{1/2}(\Gamma^s)} \\ &\leq \|\mu_h^*\|_{H^{-1/2}(\Gamma^s)} \, |v_h^s|_{1,\Omega^s} \end{aligned}$$

that, since $|\varphi_\delta|_{H^{1/2}(\Gamma^s)} = |\varphi_\delta - \breve{\varphi}^s|_{H^{1/2}(\Gamma^s)} \simeq \|\varphi_\delta - \breve{\varphi}^s\|_{H^{1/2}(\Gamma^s)}$, joined with (49) immediately implies (26).

We can collect the previous results, together with the abstract error estimates of the previous section, in the following theorem.

Theorem 3. *Assume that the assumptions on the decompositions $\mathcal{T}_\delta^\Sigma$ and $\mathcal{T}_h^s$ of Section 2 are satisfied, and assume that the spaces Φ_δ, M_h^s and V_h^s are defined as in* (43), (44) *and* (18) *with* (45), *respectively. Assume finally that* (48) *holds. Then we have*

$$|||u_h - u||| \leq C\,(|h|^k + |\delta|^k)\|u\|_{k+1,\Omega} \tag{51}$$

The proof follows immediately from Theorem 1, the results of this section, and usual approximation estimates.

We end this section with some observations on the actual implementation of the method when the bubble stabilization (45) is used.

Indeed, let us see how the computation of the generation operators $\mathcal{G}^s$ can be performed in practice. Assume that we are given a function φ in, say, $L^2(\Gamma^s)$. We recall that, to compute $\widetilde{\theta_h^s} = \mathcal{G}^s(\varphi)$, we have to find the pair $(\widetilde{\theta_h^s}, \widetilde{\mu_h^s}) \in \Theta_h^s \times M_h^s$ such that

$$\int_{\Gamma^s} (\varphi - \widetilde{\theta_h^s})\,\mu_h^s \,\mathrm{d}x = 0 \qquad \forall \mu_h^s \in M_h^s, \tag{52}$$

$$\sum_{T \in \mathcal{T}_h^{\Gamma^s}} \int_T h_T^{-1} (\varphi - \widetilde{\theta_h^s})\,\theta_h^s \,\mathrm{d}x + \int_{\Gamma^s} \widetilde{\mu_h^s}\,\theta_h^s \,\mathrm{d}x = 0 \qquad \forall \theta_h^s \in \Theta_h^s. \tag{53}$$

We also recall that, with the choice (45), the space Θ_h^s can be written as $\Theta_h^s = \mathcal{L}_k^1(\mathcal{T}_h^{\Gamma^s}) + B_{k+2}(\mathcal{T}_h^{\Gamma^s})$ where $\mathcal{L}_k^1(\mathcal{T}_h^{\Gamma^s})$ is, as before, the space of continuous piecewise polynomials of degree k on the mesh $\mathcal{T}_h^{\Gamma^s}$, and $B_{k+2}(\mathcal{T}_h^{\Gamma^s})$ is the space of bubbles of degree $k+2$, always on $\mathcal{T}_h^{\Gamma^s}$. In order to write is as a *direct sum* we introduce the space

$$W^s = \{\theta_h^s \in \Theta_h^s \text{ such that } \int_{\Gamma^s} \theta_h^s\,\mu_h^s \mathrm{d}x = 0\ \forall \mu_h^s \in M_h^s\} \tag{54}$$

We can then split *in a unique way* $\widetilde{\theta_h^s} = \widetilde{w} + \widetilde{b}$ with $\widetilde{w} \in W^s$ and $\widetilde{b}$ in $B_{k+2}(\mathcal{T}_h^{\Gamma^s})$. It is now clear that $\widetilde{b}$ can be computed immediately from (52) that becomes:

$$\int_{\Gamma^s} (\varphi - \widetilde{b})\,\mu_h^s \,\mathrm{d}x = 0 \qquad \forall \mu_h^s \in M_h^s. \tag{55}$$

Once $\widetilde{b}$ is known, one can compute $\widetilde{w}$ from (53) that easily implies

$$\sum_{T \in \mathcal{T}_h^{\Gamma^s}} \int_T h_T^{-1} (\varphi - \widetilde{w})\,w, \mathrm{d}x = \sum_{T \in \mathcal{T}_h^{\Gamma^s}} \int_T h_T^{-1} \widetilde{b}\,w, \mathrm{d}x \qquad \forall w \in W^s. \tag{56}$$

In this way the saddle point problem (52)-(53) splits into two smaller subproblems, each with a symmetric and positive definite matrix. In particular (55) can be solved element by element, so that (56) is the only true system to be solved.

5 Relaxing the continuity of the *Mothers*

One of the main advantages of the present method (and in general of all non conforming domain decomposition methods) is the freedom given by the possibility of meshing and treating each sub-domain independently of the others. In our approach however, the discretization Φ_δ of $H^{1/2}(\Sigma)$ is required to be continuous. Such request can be relaxed by defining Φ_δ face by face and asking for continuity within each face but allowing the elements of Φ_δ to jump across the boundary between two adjacent faces. More precisely, considering a splitting of the skeleton Σ in disjoint faces $\Sigma = \cup f$ (with $f = \Gamma^s \cap \Gamma^\ell$ for some $s, \ell = 1, \ldots, S$) we can introduce for each face a family of triangulations $\mathcal{T}_\delta^f$ and consider a corresponding space $\Phi_\delta^f \subset H^{1/2}(f)$ of piecewise polynomials. The global space Φ_δ could then be defined by

$$\Phi_\delta = \{\varphi_\delta \in L^2(\Sigma) \text{ with } \varphi_\delta|_f \in \Phi_\delta^f \text{ for all faces } f \text{ of } \Sigma\}.$$

Such a choice has several advantages, in particular from the point of view of implementation. Each face can be meshed independently of the other faces. Moreover, each node on Σ belongs to only one face f and therefore it only "sees" two sub-domains. This greatly simplifies the data structure needed for describing the elements of Φ_δ and the manipulations of such elements and of their interaction with other elements.

The analysis presented in the previous section needs then to be modified in order to take the discontinuity of the mothers into account. In particular, if the elements of Φ_δ are discontinuous, the space Φ_δ is not a subspace of $H^{1/2}(\Sigma)$, and therefore bounds like $\|\mathcal{G}^s(u - \psi_I)\|_{H^{1/2}(\Gamma^s)} \leq \|u - \psi_I\|_{H^{1/2}(\Gamma^s)}$ would not make sense. A completely revised analysis is carried out in a further work in preparation, and results in an almost optimal estimate (with the loss of a logarithmic factor). We just point out that the analysis of Section 3 could still be applied if the space $\Phi_\delta^c = \Phi_\delta \cap H^{1/2}(\Sigma)$ has good approximation properties. Such space is the one where one should choose the best approximation ψ_I. This is indeed a very special case: in general such space does not provide a good approximation. It may very well happen that it contains only the function $\varphi_\delta = 0$. A case in which the space Φ_δ^c does provide good approximation is the case in which the meshes on two adjacent faces share a sufficiently fine set of common nodes (in particular the case when, restricted to the common edge, the nodes of the two (or more) meshes are one a subset of the other). Though this is quite an heavy restriction to the freedom given by the possibility of using discontinuous mothers, such a case would still have many advantages from the implementation point of view, while retaining the optimal error estimate. Remark that the subspace Φ_δ^c would only be used for analyzing the method, while its implementation fully relies on the discontinuous space Φ_δ.

References

I. Babuska. The finite element method with lagrangian multipliers. *Numer. Math.*, 20:179–192, 1973.

C. Baiocchi, F. Brezzi, and L. D. Marini. Stabilization of galerkin methods and applications to domain decomposition. In A. Bensoussan et al., editor, *Future Tendencies in Computer Science, Control and Applied Mathematics*, volume 653 of *Lecture Notes in Computer Science*, pages 345–355. Springer-Verlag, 1992.

F. B. Belgacem and Y. Maday. The mortar element method for three dimensional finite elements. *RAIRO Mathematical Modelling and Numerical Analysis*, 31(2):289–302, 1997.

C. Bernardi, Y. Maday, and A. T. Patera. Domain decomposition by the mortar element method. In H. K. ans M. Garbey, editor, *Asymptotic and Numerical Methods for Partial Differential Equations with Critical Parameters*, pages 269–286. N.A.T.O. ASI, Kluwer Academic Publishers, 1993.

C. Bernardi, Y. Maday, and F. Rapetti. *Discrétisations variationnelles de problèmes aux limites elliptiques*. Mathématiques et Applications. SMAI, to appear.

S. Bertoluzza. Analysis of a stabilized three-fields domain decomposition method. *Numer. Math.*, 93(4):611–634, 2003. ISSN 0029-599X.

F. Brezzi and M. Fortin. *Mixed and Hybrid Finite Element Methods*. Springer-Verlag, New-York, 1991a.

F. Brezzi and M. Fortin. *Mixed and hybrid finite element methods*. Springer-Verlag, New York, 1991b. ISBN 0-387-97582-9.

F. Brezzi, L. P. Franca, L. D. Marini, and A. Russo. Stabilization techniques for domain decomposition methods with nonmatching grids. In *Proc. from the IX International Conference on Domain Decomposition Methods, June 1996, Bergen, Norway*, 1997.

F. Brezzi and L. D. Marini. A three field domain decomposition method. *Contemp. Math.*, 157:27–34, 1994.

F. Brezzi and L. D. Marini. Error estimates for the three-field formulation with bubble stabilization. *Math. of Comp.*, 70:911–934, 2000.

A. Buffa. Error estimates for a stabilized domain decomposition method with nonmatching grids. *Numer. Math.*, 90(4):617–640, 2002.

P. Clément. Approximation by finite element functions using local regularization. *RAIRO Anal. Numér.*, 9:77–84, 1975.

R. Hoppe, Y. Iliash, Y. Kuznetsov, Y. Vassilevski, and B. Wohlmuth. Analysis and parallel implementation of adaptive mortar element methods. *East West J. Num. An.*, 6(3):223–248, 1998.

B. Wohlmuth. *Discretization Methods and Iterative Solvers Based on Domain Decomposition*, volume 17 of *Lecture Notes in Computational Science and Engineering*. Springer, 2001.

A FETI Method for a Class of Indefinite or Complex Second- or Fourth-Order Problems

Charbel Farhat[1], Jing Li[2], Michel Lesoinne[1], and Philippe Avery[1]

[1] University of Colorado at Boulder, Department of Aerospace Engineering Sciences (`http://caswww.colorado.edu/~charbel/`)
[2] Kent State University, Department of Mathematical Sciences

Summary. The FETI-DP domain decomposition method is extended to address the iterative solution of a class of indefinite problems of the form $(\mathbf{K} - \sigma^2\mathbf{M})\mathbf{x} = \mathbf{b}$, and a class of complex problems of the form $(\mathbf{K} - \sigma^2\mathbf{M} + i\sigma\mathbf{D})\mathbf{x} = \mathbf{b}$, where $\mathbf{K}$, $\mathbf{M}$, and $\mathbf{D}$ are three real symmetric positive semi-definite matrices arising from the finite element discretization of either second-order elastodynamic problems or fourth-order plate and shell dynamic problems, i is the imaginary complex number, and σ is a positive real number.

1 Introduction

Real linear or linearized systems of equations of the form

$$(\mathbf{K} - \sigma^2\mathbf{M})\mathbf{x} = \mathbf{b} \tag{1}$$

and complex linear or linearized systems of equations of the form

$$(\mathbf{K} - \sigma^2\mathbf{M} + i\sigma\mathbf{D})\mathbf{x} = \mathbf{b} \tag{2}$$

are frequent in computational structural dynamics. Eq. (1) is encountered, for example, in the finite element (FE) simulation of the forced response of an undamped mechanical system to a periodic excitation . In that case, $\mathbf{K}$ and $\mathbf{M}$ are the FE stiffness and mass matrices of the considered mechanical system, respectively, σ is the circular frequency of the external periodic excitation, $\mathbf{b}$ is its amplitude, $(\mathbf{K} - \sigma^2\mathbf{M})$ is the impedance of the mechanical system, and $\mathbf{x}$ is the amplitude of its forced response. Such problems also arise during the solution by an inverse shifted method of the generalized symmetric eigenvalue problem $\mathbf{K}\mathbf{x} = \omega^2\mathbf{M}\mathbf{x}$ associated with an undamped mechanical system. In that example, $\mathbf{K}$ and $\mathbf{M}$ have the same meaning as in the previous case, (ω^2, $\mathbf{x}$) is a desired pair of eigenvalue and eigenvector representing the square of a natural circular frequency and the corresponding natural vibration mode of the undamped mechanical system, respectively, and the shift σ^2 is introduced

to obtain quickly the closest eigenvalues to σ^2. In both examples mentioned here, the matrices $\mathbf{K}$ and $\mathbf{M}$ are symmetric positive semi-definite, and therefore $(\mathbf{K} - \sigma^2\mathbf{M})$ rapidly becomes indefinite when σ is increased. Eq. (2) is encountered in similar problems when the mechanical system is damped, in which case i denotes the pure imaginary number satisfying $i^2 = -1$ and $\mathbf{D}$ denotes the FE damping matrix and is also symmetric positive semi-definite.

Domain decomposition based preconditioned conjugate gradient (PCG) methods have emerged as powerful equation solvers in this field on both sequential and parallel computing platforms. While most successful domain decomposition methods (DDMs) have been designed for the solution of symmetric positive (semi-) definite systems, some have targeted indefinite problems of the form given in (1) (Cai and Widlund [1992]) . The objective of this paper is to present an alternative DDM that addresses both classes of indefinite (1) and complex (2) problems, that is based on the FETI-DP (Farhat, Lesoinne and Pierson [2000], Farhat et al. [2001]) DDM, and that is scalable when $\mathbf{K}$, $\mathbf{M}$, and $\mathbf{D}$ result from the FE discretization of second-order elastodynamic problems and fourth-order plate and shell dynamic problems.

2 The FETI-DP method

The dual-primal finite element tearing and interconnecting method (FETI-DP) (Farhat, Lesoinne and Pierson [2000], Farhat et al. [2001]) is a third-generation FETI method (for example, see Farhat [1991], Farhat and Roux [1991]) developed for the scalable and fast iterative solution of systems of equations arising from the FE discretization of static, dynamic, second-order, and fourth-order elliptic partial differential equations (PDEs). When equipped with the Dirichlet preconditioner (Farhat, Mandel and Roux [1994]) and applied to fourth-order or two-dimensional second-order problems, the condition number κ of its interface problem grows asymptotically as (Mandel and Tezaur [2001])

$$\kappa = \mathcal{O}\ (1 + \log^m \frac{H}{h}\ ), \quad m \leq 2, \tag{3}$$

where H and h denote the subdomain and mesh sizes, respectively. When equipped with the same Dirichlet preconditioner and an auxiliary coarse problem constructed by enforcing some set of optional constraints at the subdomain interfaces (Farhat et al. [2001]), the condition number estimate (3) also holds for second-order scalar elliptic problems (Klawonn, Widlund and Dryja [2002]). The result (3) proves the numerical scalability of the FETI methodology with respect to all of the problem size, the subdomain size, and the number of subdomains. More specifically, it suggests that one can expect the FETI-DP method to solve small-scale and large-scale problems in similar iteration counts. This in turn suggests that when the FETI-DP method is well-implemented on a parallel processor, it should be capable of solving an n-times larger problem using an n-times larger number of processors in almost

a constant CPU time. This was demonstrated in practice for many complex structural mechanics problems (for example, see Farhat, Lesoinne and Pierson [2000] and Farhat et al. [2001] and the references cited therein).

Next, the FETI-DP method is overviewed in the context of the generic symmetric positive semi-definite (static) problem

$$\mathbf{K}\mathbf{x} = \mathbf{b}, \tag{4}$$

where $\mathbf{K}$ has the same meaning as in problems (1,2) and $\mathbf{b}$ is an arbitrary vector, in order to keep this paper as self-contained as possible.

2.1 Non-overlapping domain decomposition and notation

Let Ω denote the computational support of a second- or fourth-order problem whose discretization leads to problem (4), $\{\Omega^{(s)}\}_{s=1}^{N_s}$ denote its decomposition into N_s subdomains with matching interfaces $\Gamma^{(s,q)} = \partial\Omega^{(s)} \bigcap \partial\Omega^{(q)}$, and let $\Gamma = \bigcup_{s=1,q>s}^{s=N_s} \Gamma^{(s,q)}$ denote the global interface of this decomposition. *In the remainder of this paper, each interface $\Gamma^{(s,q)}$ is referred to as an "edge", whether Ω is a two- or three-dimensional domain.* Let also $\mathbf{K}^{(s)}$ and $\mathbf{b}^{(s)}$ denote the contributions of subdomain $\Omega^{(s)}$ to $\mathbf{K}$ and $\mathbf{b}$, respectively, and let $\mathbf{x}^{(s)}$ denote the vector of dof associated with it.

Let N_c of the N_I nodes lying on the global interface Γ be labeled "corner" nodes (see Fig. 1), Γ_c denote the set of these corner nodes, and let $\Gamma' = \Gamma \backslash \Gamma_c$. If in each subdomain $\Omega^{(s)}$ the unknowns are partitioned into global corner dof designated by the subscript c, and "remaining" dof designated by the subscript r, $\mathbf{K}^{(s)}$, $\mathbf{x}^{(s)}$ and $\mathbf{b}^{(s)}$ can be partitioned as follows

$$\mathbf{K}^{(s)} = \begin{bmatrix} \mathbf{K}_{rr}^{(s)} & \mathbf{K}_{rc}^{(s)} \\ \mathbf{K}_{rc}^{(s)^T} & \mathbf{K}_{cc}^{(s)} \end{bmatrix}, \qquad \mathbf{x}^{(s)} = \begin{bmatrix} \mathbf{x}_r^{(s)} \\ \mathbf{x}_c^{(s)} \end{bmatrix} \qquad \text{and} \qquad \mathbf{b}^{(s)} = \begin{bmatrix} \mathbf{b}_r^{(s)} \\ \mathbf{b}_c^{(s)} \end{bmatrix}. \tag{5}$$

The r-type dof can be further partitioned into "interior" dof designated by the subscript i, and subdomain interface "boundary" dof designated by the subscript b. Hence, $\mathbf{x}_r^{(s)}$ and $\mathbf{b}_r^{(s)}$ can be further partitioned as follows

$$\mathbf{x}_r^{(s)} = \begin{bmatrix} \mathbf{x}_i^{(s)} & \mathbf{x}_b^{(s)} \end{bmatrix}^T \qquad \text{and} \qquad \mathbf{b}_r^{(s)} = \begin{bmatrix} \mathbf{b}_i^{(s)} & \mathbf{b}_b^{(s)} \end{bmatrix}^T, \tag{6}$$

where the superscript T designates the transpose.

Let $\mathbf{x}_c$ denote the global vector of corner dof, and $\mathbf{x}_c^{(s)}$ denote its restriction to $\Omega^{(s)}$. Let also $\mathbf{B}_r^{(s)}$ and $\mathbf{B}_c^{(s)}$ be the two subdomain Boolean matrices defined by

$$\mathbf{B}_r^{(s)}\mathbf{x}_r^{(s)} = \pm\mathbf{x}_b^{(s)} \qquad \text{and} \qquad \mathbf{B}_c^{(s)}\mathbf{x}_c = \mathbf{x}_c^{(s)}, \tag{7}$$

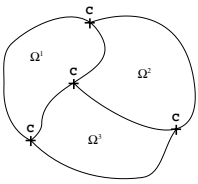

Fig. 1. Example of a definition of corner points

where the $\pm$ sign is set by any convention that implies that $\sum_{s=1}^{N_s} \mathbf{B}_r^{(s)} \mathbf{x}_r^{(s)}$ represents the *jump* of the solution $\mathbf{x}$ across the subdomain interfaces. Finally, let

$$\mathbf{b}_c = \sum_{s=1}^{N_s} \mathbf{B}_c^{(s)^T} \mathbf{b}_c^{(s)}. \tag{8}$$

In Farhat, Lesoinne and Pierson [2000] and Farhat et al. [2001], it was shown that solving problem (4) is equivalent to solving the following domain-decomposed problem

$$\mathbf{K}_{rr}^{(s)} \ \mathbf{x}_r^{(s)} + \mathbf{K}_{rc}^{(s)} \mathbf{B}_c^{(s)} \ \mathbf{x}_c + \mathbf{B}_r^{(s)^T} \lambda + \mathbf{B}_r^{(s)^T} \mathbf{Q}_b \ \mu = \mathbf{b}_r^{(s)}, \quad s = 1, ..., N_s \tag{9}$$

$$\sum_{s=1}^{N_s} \mathbf{B}_c^{(s)^T} \mathbf{K}_{rc}^{(s)^T} \ \mathbf{x}_r^{(s)} + \sum_{s=1}^{N_s} \mathbf{B}_c^{(s)^T} \mathbf{K}_{cc}^{(s)} \mathbf{B}_c^{(s)} \ \mathbf{x}_c = \mathbf{b}_c, \tag{10}$$

$$\sum_{s=1}^{N_s} \mathbf{B}_r^{(s)} \mathbf{x}_r^{(s)} = 0, \tag{11}$$

$$\mathbf{Q}_b^T \sum_{s=1}^{N_s} \mathbf{B}_r^{(s)} \mathbf{x}_r^{(s)} = 0, \tag{12}$$

where λ is an N_λ-long vector of Lagrange multipliers introduced on Γ' to enforce the continuity (11) of the solution $\mathbf{x}$, and μ is another vector of Lagrange multipliers introduced to enforce the optional linear constraints (12). These optional constraints, a concept first developed in Farhat, Chen, Risler and Roux [1998], are associated with a matrix $\mathbf{Q}_b$ with $N_Q < N_\lambda$ columns defined on Γ'. The word "optional" refers to the fact that Eq. (12) and the vector of Lagrange multipliers μ are not necessarily needed for formulating the above domain-decomposed problem. Indeed, since the solution of problem (4) is continuous across the subdomain interfaces, it satisfies Eq. (11) and therefore satisfies Eq. (12) for any matrix $\mathbf{Q}_b$.

The domain-decomposed problem (9–12) was labeled "dual-primal" in Farhat, Lesoinne and Pierson [2000] and Farhat et al. [2001] because it is formulated in terms of two different types of global unknowns: the dual Lagrange multipliers represented by the vector λ, and the primal corner dof represented by the vector $\mathbf{x}_c$.

In the remainder of this paper, the j-th column of $\mathbf{Q}_b$ is denoted by $\mathbf{q}_j$.

2.2 Interface and coarse problems

Let

$$\widetilde{\mathbf{K}}_{cc} = \begin{bmatrix} \mathbf{K}_{cc} & 0 \\ 0 & 0 \end{bmatrix}, \qquad \mathbf{d}_r = \sum_{s=1}^{N_s} \mathbf{B}_r^{(s)} \mathbf{K}_{rr}^{(s)^{-1}} \mathbf{b}_r^{(s)},$$

$$\text{and} \qquad \mathbf{b}_c^* = \mathbf{b}_c - \sum_{s=1}^{N_s} (\mathbf{K}_{rc}^{(s)} \mathbf{B}_c^{(s)})^T \mathbf{K}_{rr}^{(s)^{-1}} \mathbf{b}_r^{(s)}. \tag{13}$$

After some algebraic manipulations aimed at eliminating symbolically $\mathbf{x}_r^{(s)}$, $s = 1, ..., N_s$, $\mathbf{x}_c$, and μ, the domain-decomposed problem (9–12) can be transformed into the following symmetric positive semi-definite interface problem

$$(\mathbf{F}_{I_{rr}} + \widetilde{\mathbf{F}}_{I_{rc}} \widetilde{\mathbf{K}}_{cc}^{*^{-1}} \widetilde{\mathbf{F}}_{I_{rc}}^T)\lambda = \mathbf{d}_r - \widetilde{\mathbf{F}}_{I_{rc}} \widetilde{\mathbf{K}}_{cc}^{*^{-1}} \tilde{\mathbf{b}}_c^*, \tag{14}$$

where

$$\mathbf{F}_{I_{rr}} = \sum_{s=1}^{N_s} \mathbf{B}_r^{(s)} \mathbf{K}_{rr}^{(s)^{-1}} \mathbf{B}_r^{(s)^T}, \qquad \widetilde{\mathbf{F}}_{I_{rc}} = \sum_{s=1}^{N_s} \mathbf{B}_r^{(s)} \mathbf{K}_{rr}^{(s)^{-1}} \widetilde{\mathbf{K}}_{rc}^{(s)} \mathbf{B}_c^{(s)},$$

$$\widetilde{\mathbf{K}}_{rc}^{(s)} = \left[\mathbf{K}_{rc}^{(s)} \mathbf{B}_c^{(s)} \quad \mathbf{B}_r^{(s)^T} \mathbf{Q}_b \right], \qquad \tilde{\mathbf{b}}_c^* = \begin{bmatrix} \mathbf{b}_c^* \\ -\mathbf{Q}_b^T \mathbf{d}_r \end{bmatrix},$$

$$\widetilde{\mathbf{K}}_{cc}^* = \widetilde{\mathbf{K}}_{cc} - \begin{bmatrix} \sum_{s=1}^{N_s} (\mathbf{K}_{rc}^{(s)} \mathbf{B}_c^{(s)})^T \mathbf{K}_{rr}^{(s)^{-1}} (\mathbf{K}_{rc}^{(s)} \mathbf{B}_c^{(s)}) & \sum_{s=1}^{N_s} (\mathbf{K}_{rc}^{(s)} \mathbf{B}_c^{(s)})^T \mathbf{K}_{rr}^{(s)^{-1}} (\mathbf{B}_r^{(s)^T} \mathbf{Q}_b) \\ \sum_{s=1}^{N_s} (\mathbf{B}_r^{(s)^T} \mathbf{Q}_b)^T \mathbf{K}_{rr}^{(s)^{-1}} (\mathbf{K}_{rc}^{(s)} \mathbf{B}_c^{(s)}) & \sum_{s=1}^{N_s} (\mathbf{B}_r^{(s)^T} \mathbf{Q}_b)^T \mathbf{K}_{rr}^{(s)^{-1}} (\mathbf{B}_r^{(s)^T} \mathbf{Q}_b) \end{bmatrix}. \tag{15}$$

The FETI-DP method is a DDM which solves the original problem (4) by applying a PCG algorithm to the solution of the corresponding dual interface problem (14). At the n-th PCG iteration, the matrix-vector product $(\mathbf{F}_{I_{rr}} + \widetilde{\mathbf{F}}_{I_{rc}} \widetilde{\mathbf{K}}_{cc}^{*^{-1}} \widetilde{\mathbf{F}}_{I_{rc}}^T)\lambda^n$ incurs the solution of an auxiliary problem of the form

$$\widetilde{\mathbf{K}}_{cc}^* \mathbf{z} = \widetilde{\mathbf{F}}_{I_{rc}}^T \lambda^n. \tag{16}$$

From the fifth of Eqs. (15), it follows that the size of this auxiliary problem is equal to the sum of the number of corner dof, N_c^{dof}, and the number of columns of the matrix $\mathbf{Q}_b$, N_Q.

For $N_Q = 0$ — that is, for $\mathbf{Q}_b = 0$, the auxiliary problem (16) is a coarse problem, and $\widetilde{\mathbf{K}}_{cc}^*$ is a sparse matrix whose pattern is that of the stiffness matrix obtained when each subdomain is treated as a "superelement" whose nodes are its corner nodes. This coarse problem ensures that the FETI-DP method equipped with the Dirichlet preconditioner (see Section 2.3) is numerically scalable for fourth-order plate and shell problems, and two-dimensional

second-order elasticity problems (Farhat et al. [2001], Mandel and Tezaur [2001]). However, for $\mathbf{Q}_b = 0$, the FETI-DP method equipped with the Dirichlet preconditioner is not numerically scalable for three-dimensional second-order problems.

For any choice of $\mathbf{Q}_b \neq 0$, $\widetilde{\mathbf{K}}^*_{cc}$ remains a sparse matrix. If $\mathbf{Q}_b$ is constructed edge-wise — that is, if each column of $\mathbf{Q}_b$ is constructed as the restriction of some operator to a specific edge of Γ' — the sparsity pattern of $\widetilde{\mathbf{K}}^*_{cc}$ becomes that of a stiffness matrix obtained by treating each subdomain as a superelement whose nodes are its corner nodes augmented by virtual mid-side nodes. The number of dof attached to each virtual mid-side node is equal to the number of columns of $\mathbf{Q}_b$ associated with the edge on which lies this mid-side node. If N_Q is kept relatively small, the auxiliary problem (16) remains a relatively small coarse problem. This coarse problem was labeled "augmented" coarse problem in Farhat, Lesoinne and Pierson [2000] in order to distinguish it from the smaller coarse problem obtained with $\mathbf{Q}_b = 0$. Furthermore, each column of $\mathbf{Q}_b$ is referred to as an "augmentation coarse mode". When these augmentation coarse modes are chosen as the translational rigid body modes of each edge of Γ', the FETI-DP method equipped with the Dirichlet preconditioner becomes numerically scalable for three-dimensional second-order problems (Klawonn, Widlund and Dryja [2002]).

2.3 Local preconditioning

Two local preconditioners have been developed so far for the FETI-DP method:

1. The Dirichlet preconditioner which can be written as

$$\overline{\mathbf{F}}^{D^{-1}}_{I_{rr}} = \sum_{s=1}^{N_s} \mathbf{W}^{(s)} \mathbf{B}^{(s)}_r \begin{bmatrix} 0 & 0 \\ 0 & \mathbf{S}^{(s)}_{bb} \end{bmatrix} \mathbf{B}^{(s)^T}_r \mathbf{W}^{(s)},$$

$$\text{where} \qquad \mathbf{S}^{(s)}_{bb} = \mathbf{K}^{(s)}_{bb} - \mathbf{K}^{(s)^T}_{ib} \mathbf{K}^{(s)^{-1}}_{ii} \mathbf{K}^{(s)}_{ib}, \tag{17}$$

   the subscripts i and b have the same meaning as in Section 2.1, and $\mathbf{W}^{(s)}$ is a subdomain diagonal scaling matrix that accounts for possible subdomain heterogeneities (Rixen and Farhat [1999]). This preconditioner is mathematically optimal in the sense that it leads to the condition number estimate (3).
2. The lumped preconditioner which can be written as

$$\overline{\mathbf{F}}^{L^{-1}}_{I_{rr}} = \sum_{s=1}^{N_s} \mathbf{W}^{(s)} \mathbf{B}^{(s)}_r \begin{bmatrix} 0 & 0 \\ 0 & \mathbf{K}^{(s)}_{bb} \end{bmatrix} \mathbf{B}^{(s)^T}_r \mathbf{W}^{(s)}. \tag{18}$$

   This preconditioner is not mathematically optimal in the sense defined above; however, it decreases the cost of each iteration in comparison with the Dirichlet preconditioner often with a modest increase in the iteration count.

3 The FETI-DPH method

In the context of Eq. (1), $\mathbf{K}_{rr}^{(s)}$ becomes $\mathbf{K}_{rr}^{(s)} - \sigma^2\mathbf{M}_{rr}^{(s)}$. Hence, the extension of the FETI-DP method to problems of the form given in (1) or (2) requires addressing the following issues:

1. $\mathbf{K}_{rr}^{(s)} - \sigma^2\mathbf{M}_{rr}^{(s)}$ is indefinite and therefore the dual interface problem (14) is indefinite.
2. Independently of which interface points are chosen as corner points, $\mathbf{K}_{rr}^{(s)} - \sigma^2\mathbf{M}_{rr}^{(s)}$ is in theory singular when σ^2 coincides with an eigenvalue of the pencil $(\mathbf{K}_{rr}^{(s)}, \mathbf{M}_{rr}^{(s)})$.
3. How to construct augmentation coarse modes and extended Dirichlet and lumped preconditioners that address the specifics of problems (1,2).

For problems of the form given in (2), only the third issue is relevant. The first issue can be addressed by solving the dual interface problem (14) by a preconditioned generalized minimum residual (PGMRES) algorithm rather than a PCG algorithm. The second and third issues were addressed in Farhat, Macedo and Lesoinne [2000] in the context of the basic FETI method and acoustic scattering applications — that is, for the exterior Helmholtz *scalar* problem where $\sigma^2 = k^2$ and k denotes the wave number. More specifically, a regularization procedure was developed in that reference to prevent all subdomain problems from being singular for any value of the wave number k, without destroying the sparsity of the local matrices $\mathbf{K}_{rr}^{(s)} - k^2\mathbf{M}_{rr}^{(s)}$ and without affecting the solution of the original problem (1). Furthermore, for the scalar Helmholtz equation, the coarse modes were chosen in Farhat, Macedo and Lesoinne [2000] as plane waves of the form $e^{ik\theta_j^T X_b}$, $j = 1, 2, \cdots$, where θ_j denotes a direction of wave propagation and X_b the coordinates of a node on Γ. The resulting DDM was named the FETI-H method (H for Helmholtz).

Unfortunately, the regularization procedure characterizing the FETI-H method transforms each real subdomain problem associated with Eq. (1) into a complex subdomain problem. For acoustic scattering applications, this is not an issue because the Sommerfeld radiation condition causes the original problem to be in the complex domain. However, for real-valued problems such as those represented by Eq. (1), the regularization procedure of the FETI-H method is unjustifiable from computational resource and performance viewpoints.

In practice, experience reveals that $\mathbf{K}_{rr}^{(s)} - \sigma^2\mathbf{M}_{rr}^{(s)}$ is non-singular as long as $\mathbf{K}_{rr}^{(s)}$ is non-singular. This observation is exploited here to design an extension of the FETI-DP method for indefinite problems of the form given in (1) and complex problems of the form given in (2) by:

1. Replacing the PCG solver by the PGMRES solver.
2. Adapting the Dirichlet and lumped preconditioners to exploit an interesting characteristic of problems (1,2).

3. Constructing a new augmentation coarse space that is effective for second-order elastodynamic problems as well as fourth-order plate and shell dynamic problems.

The extension of FETI-DP outlined above is named here the FETI-DPH method.

3.1 Adapted Dirichlet and lumped preconditioners

Consider the subdomain (impedance) matrix

$$\mathbf{Z}_{rr}^{(s)} = \mathbf{K}_{rr}^{(s)} - \sigma^2 \mathbf{M}_{rr}^{(s)}. \tag{19}$$

For the applications outlined in the introduction, $\mathbf{M}_{rr}^{(s)}$ is a mass matrix; hence, in three dimensions and at the element level, this matrix is proportional to h^3. On the other hand, for the same applications, $\mathbf{K}_{rr}^{(s)}$ is a stiffness matrix; in three dimensions and at the element level, it is proportional to h for second-order elasticity problems, and to $1/h^2$ for fourth-order plate and shell problems. It follows that for a sufficiently fine mesh, $\mathbf{Z}_{rr}^{(s)}$ is dominated by $\mathbf{K}_{rr}^{(s)}$. These observations, the optimality of the Dirichlet preconditioner and the computational efficiency of the lumped preconditioner established for the solution of problem (4) suggest preconditioning the local matrices $\mathbf{Z}_{rr}^{(s)}$ by Dirichlet and lumped constructs that are based on $\mathbf{K}_{rr}^{(s)}$ (see Section 2.3) and not $\mathbf{Z}_{rr}^{(s)}$. When Rayleigh damping is used,

$$\mathbf{D}_{rr}^{(s)} = c_K \mathbf{K}_{rr}^{(s)} + c_M \mathbf{M}_{rr}^{(s)}, \tag{20}$$

where c_K and c_M are two real constants, and the same reasoning can be invoked to advocate preconditioning the local matrices

$$\mathbf{Z}_{rr}^{(s)} = \mathbf{K}_{rr}^{(s)} - \sigma^2 \mathbf{M}_{rr}^{(s)} + i\sigma \mathbf{D}_{rr}^{(s)} \tag{21}$$

by Dirichlet and lumped constructs that are based on $(1 + i\sigma c_K)\mathbf{K}_{rr}^{(s)}$ and not $\mathbf{Z}_{rr}^{(s)}$.

Finally, it is pointed out that the ad-hoc reasoning outlined above can be mathematically justified, at least in the context of the scalar Helmholtz equation (for example, see Klawonn [1995] and the references cited therein).

3.2 Wavy augmented coarse problem

Let $\mathbf{r}$ denote the residual associated with the iterative solution of the dual interface problem (14). From Eqs. (9–12) and Eq. (14), it follows that

$$\mathbf{r} = \mathbf{d}_r - \widetilde{\mathbf{F}}_{I_{rc}} \widetilde{\mathbf{K}}_{cc}^{*^{-1}} \tilde{\mathbf{b}}_c^* - (\mathbf{F}_{I_{rr}} + \widetilde{\mathbf{F}}_{I_{rc}} \widetilde{\mathbf{K}}_{cc}^{*^{-1}} \widetilde{\mathbf{F}}_{I_{rc}}^T)\lambda = \sum_{s=1}^{N_s} \mathbf{B}_r^{(s)} \mathbf{x}_r^{(s)}, \tag{22}$$

which shows that the residual $\mathbf{r}$ represents the jump of the iterate solution across the subdomain interfaces.

From Eq. (12), Eq. (15), Eq. (14) and Eq. (11), it follows that at each iteration of the PGMRES algorithm applied to the solution of problem (14), FETI-DPH forces the jump of the solution across the subdomain interfaces to be orthogonal to the subspace represented by the matrix $\mathbf{Q}_b$. This feature is a strategy for designing an auxiliary coarse problem which, when $\mathbf{Q}_b$ is well chosen, accelerates the convergence of a DDM (Farhat, Chen, Risler and Roux [1998]). In this work, the search for a suitable matrix $\mathbf{Q}_b$ is driven by the following reasoning. Suppose that the space of traces on Γ' of the desired solution of problem (1) is spanned by a set of orthogonal vectors $\{\mathbf{v}_{j_E}\}_{j=1}^{N_\lambda}$, where the subscript E indicates that $\mathbf{v}_{j_E}$ is non-zero only on edge $E \in \Gamma'$. Then, the residual $\mathbf{r}$ defined in Eq. (22) can be written as

$$\mathbf{r} = \sum_{j=1}^{N_\lambda} \alpha_j \mathbf{v}_{j_E}, \tag{23}$$

where $\{\alpha_j\}_{j=1}^{N_\lambda}$ is a set of real coefficients. If each augmentation coarse mode is chosen as

$$\mathbf{q}_j = \mathbf{v}_{j_E}, \qquad j = 1, \cdots, N_Q, \tag{24}$$

Eq. (12) simplifies to

$$\alpha_j = 0, \qquad j = 1, \cdots, \ N_Q. \tag{25}$$

In that case, Eq. (25) implies that at each iteration of the PGMRES algorithm, the first N_Q components of the residual $\mathbf{r}$ in the basis $\{\mathbf{v}_{j_E}\}_{j=1}^{N_\lambda}$ are zero. If a few vectors $\{\mathbf{v}_{j_E}\}_{j=1}^{N_Q}$, $N_Q << N_\lambda$, that dominate the expansion (23) can be found, then choosing these vectors as coarse augmentation modes can be expected to accelerate the convergence of the iterative solution of the dual interface problem (14). Hence, it remains to exhibit such a set of orthogonal vectors $\mathbf{v}_{j_E}$ and construct a computationally efficient matrix $\mathbf{Q}_b$.

A second-order elastodynamic problem is governed by Navier's displacement equations of motion

$$\mu \Delta u + (\Lambda + \mu) \nabla (\nabla \cdot u) + b = \rho \frac{\partial^2 u}{\partial t^2}, \tag{26}$$

where $u \in \mathbb{R}^3$ denotes the displacement (vector) field of the elastodynamic system, Λ and μ its Lamé moduli, $b \in \mathbb{R}^3$ its body forces, ρ its density, and t denotes time. If a harmonic motion is assumed, — that is, if

$$u(X, t) = v(X) e^{-i\omega t}, \tag{27}$$

where $X \in \mathbb{R}^3$ denotes the spatial variables, and ω denotes a circular frequency, the homogeneous form of Eq. (26) becomes

$$\mu \Delta v + (\Lambda + \mu)\nabla(\nabla \cdot v) + \rho\omega^2 v = 0. \tag{28}$$

The free-space solutions of the above vector equation are

$$v = a_p \sin(k_p \theta \cdot X), \quad v = a_p \cos(k_p \theta \cdot X), \tag{29}$$

$$v = a_{s_1} \sin(k_s \theta \cdot X), \quad v = a_{s_1} \cos(k_s \theta \cdot X), \tag{30}$$

$$v = a_{s_2} \sin(k_s \theta \cdot X), \quad v = a_{s_2} \cos(k_s \theta \cdot X), \tag{31}$$

where $\theta \in \mathbb{R}^3$ is an arbitrary vector of unit length ($\|\theta\|_2 = 1$), $a_p \in \mathbb{R}^3$ is a vector that is parallel to θ, $(a_{s_1}, a_{s_2}) \in \mathbb{R}^3 \times \mathbb{R}^3$ are two independent vectors in the plane orthogonal to θ,

$$k_p = \sqrt{\frac{\rho\omega^2}{\Lambda + 2\mu}}, \quad \text{and} \quad k_s = \sqrt{\frac{\rho\omega^2}{\mu}}. \tag{32}$$

The free-space solutions (29) are known as the elastic pressure or longitudinal waves, and the free-space solutions (30) and (31) are known as the elastic shear or transverse waves.

Consider next the following fourth-order PDE associated with a given elastic body

$$\Delta^2 u - \frac{m}{D}\omega^2 u = 0, \qquad \text{where} \quad m = \rho\tau, \quad D = \frac{E\tau^3}{12(1-\nu^2)}, \tag{33}$$

E denotes the Young modulus of the elastic body, ν its Poisson ratio, τ its thickness, and all other variables have the same meaning as before. The reader can check that the free-space solutions (29,30,31) with

$$k_p = k_s = \sqrt[4]{\frac{m}{D}\omega^2} \tag{34}$$

are also free-space solutions of Eq. (33). The PDE (33) can model the harmonic transverse motion of a plate. In that case, u is a scalar representing the transverse displacement field. However, for the purpose of constructing an augmented coarse problem for the FETI-DPH method, and only for this purpose, it is assumed here that when $u \in \mathbb{R}^3$, Eq. (33) models the harmonic motion of a shell in all three dimensions.

Hence, a general solution of either Eq. (28) or Eq. (33) can be written as

$$\begin{aligned} v = &\sum_{j=1}^{\infty} \left\{ a_{p_j} \left(c_{1_j} \sin(k_p \theta_j \cdot X) + c_{2_j} \cos(k_p \theta_j \cdot X) \right) \right\} \\ &+ \sum_{j=1}^{\infty} \left\{ a_{s_{1_j}} \left(c_{3_j} \sin(k_s \theta_j \cdot X) + c_{4_j} \cos(k_s \theta_j \cdot X) \right) \right\} \\ &+ \sum_{j=1}^{\infty} \left\{ a_{s_{2_j}} \left(c_{5_j} \sin(k_s \theta_j \cdot X) + c_{6_j} \cos(k_s \theta_j \cdot X) \right) \right\}, \end{aligned} \tag{35}$$

where $\theta_j \in \mathbb{R}^3$ is an arbitrary vector of unit length defining the direction of propagation of an elastic pressure or shear wave, c_{1_j}, c_{2_j}, c_{3_j}, c_{4_j}, c_{5_j}, and c_{6_j} are real coefficients, and k_p and k_s are given by Eq. (32) for a second-order elastodynamic problem and by Eq. (34) for a fourth-order plate or shell dynamic problem. From Eq. (35) and Eq. (24), it follows that the desired matrix $\mathbf{Q}_b$ is composed of blocks of six columns. The columns of each block are associated with one direction of propagation θ_j and one edge E of the mesh partition, and can be written as

$$\begin{aligned}
\mathbf{q}_{b_l} \begin{bmatrix} 3(m-1)+1 \\ 3(m-1)+2 \\ 3(m-1)+3 \end{bmatrix} &= a_{p_j} \ \sin(k_p \theta_j \cdot X_m), \\
\mathbf{q}_{b_{l+1}} \begin{bmatrix} 3(m-1)+1 \\ 3(m-1)+2 \\ 3(m-1)+3 \end{bmatrix} &= a_{p_j} \ \cos(k_p \theta_j \cdot X_m), \\
\cdots \qquad \cdots & \\
\mathbf{q}_{b_{l+4}} \begin{bmatrix} 3(m-1)+1 \\ 3(m-1)+2 \\ 3(m-1)+3 \end{bmatrix} &= a_{s_{2_j}} \sin(k_s \theta_j \cdot X_m), \\
\mathbf{q}_{b_{l+5}} \begin{bmatrix} 3(m-1)+1 \\ 3(m-1)+2 \\ 3(m-1)+3 \end{bmatrix} &= a_{s_{2_j}} \cos(k_s \theta_j \cdot X_m), \\
l = 6(j-1)+1, \qquad & m = 1, \cdots, N_I - N_c,
\end{aligned} \tag{36}$$

where $\mathbf{q}_b[3(m-1)+1]$ designates the entry of $\mathbf{q}_b$ associated with the dof in the x-direction attached to the m-th node on an edge $E \in \Gamma'$, $\mathbf{q}_b[3(m-1)+2]$ designates the entry associated with the dof along the y-direction, $\mathbf{q}_b[3(m-1)+3]$ designates the entry associated with the dof along the z-direction, and $X_m \in \mathbb{R}^3$ denotes the coordinates of this m-th node. Hence, if N_E denotes the number of edges of the mesh partition, and N_θ the number of considered directions of wave propagation, the total number of augmentation coarse modes is given in general by $N_Q = 6N_E N_\theta$. To these modes can be added the edge-based translational rigid body modes as these are free-space solutions of Eq. (28) when $\omega = 0$.

In this paper, the number of directions is limited by $N_\theta^{max} = 13$, and the directions θ_j are generated as follows. A generic cube is discretized into $3 \times 3 \times 3$ points. A direction θ_j is defined by connecting the center point to any of the other 26 points lying on a face of the cube. Since each direction θ_j is used to define both a cosine and a sine mode, only one direction θ_j is retained for each pair of opposite directions, which results in a maximum of 13 directions.

4 Performance studies and preliminary conclusions

Here, the FETI-DPH method is applied to the solution of various problems of the form given in (1) or (2) and associated with: (a) the discretization by quadratic tetrahedral elements (10 nodes per element) of a wheel carrier fixed at a few of its nodes, and (b) the discretization by linear triangular shell elements of an alloy wheel clamped at a few center points (Fig. 2). When the structure is assumed to be damped, Eq. (20) is used to construct D and c_K and c_M are determined by requiring that the critical damping ratio of the first 10 modes of the structure be equal in a least-squares sense to a specified value, ξ. In all problems, the shift is set to $\sigma^2 = \omega^2 = 4\pi^2 f^2$, where ω^2 is the square of a (possibly natural) circular frequency of the structure and f is the corresponding frequency in Hz. To help the reader appreciate the magnitude of a chosen shift value, the natural frequencies of both structures are characterized in Table 1. In order to investigate the performance, potential, and various scalability properties of the FETI-DPH method, various values of σ^2 are considered, three meshes with different resolutions are employed for the wheel carrier second-order problem (504,375 dof, 1,317,123 dof, and 2,091,495 dof), and one mesh with 936,102 dof is employed for the alloy wheel fourth-order shell problem. In all cases, the right-sides of problems (1,2) are generated by a distributed load, the computations are performed on a Silicon Graphics Origin 3800 system with 40 R12000 400 MHz processors, and convergence is declared when the relative residual satisfies

$$RE^n = \frac{\|(\mathbf{K} - \sigma^2\mathbf{M} + i\sigma\mathbf{D})\ \mathbf{x}^n - \mathbf{b}\|_2}{\|\mathbf{b}\|_\mathbf{2}} \leq 10^{-6}. \tag{37}$$

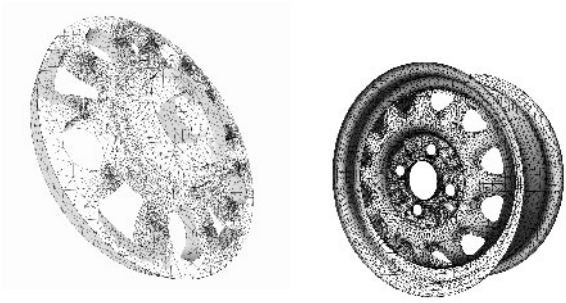

Fig. 2. FE discretizations of a wheel carrier (left) and an alloy wheel (right)

First, attention is directed to the wheel carrier undamped problem, and for each generated mesh, N_s is chosen to keep the subdomain problem size constant. Two frequencies, 500 KHz and 2 MHz, are considered: the latter value of the shift σ^2 arises, for example, when exciting the structure by its $200-th$ natural frequency, or shifting around it during the solution of an

Table 1. Eigenvalue/Frequency partial spectrum of the pencil $(\mathbf{K}, \mathbf{M})$

	Wheel Carrier	(2^{nd}-order)	Alloy Wheel	(4^{th}-order)
Mode Number	Eigenvalue (ω^2)	Frequency	Eigenvalue (ω^2)	Frequency
1	2.6e+11	8.2e+04 Hz	7.6e+05	1.4e+02 Hz
100	5.2e+13	1.1e+06 Hz	1.0e+09	5.1e+03 Hz
200	1.6e+14	2.0e+06 Hz	3.0e+09	8.7e+03 Hz
300	2.8e+14	2.6e+06 Hz	5.7e+09	1.2e+04 Hz
400	4.0e+14	3.2e+06 Hz	9.5e+09	1.5e+04 Hz
500	5.1e+14	3.5e+06 Hz		
600	6.0e+14	3.9e+06 Hz		

eigenvalue problem. The number of wave directions is set to $N_\theta = 2$, and the three translational rigid body modes are included in the construction of the augmentation matrix $\mathbf{Q}_b$. The performance results of the FETI-DPH solver obtained on $N_p = 12$ processors are reported in Table 2 where N_{itr} records the iteration count. For each considered frequency, the iteration count associated with the chosen number of subdomains and chosen preconditioner is almost independent of the mesh size, which highlights the numerical scalability of the FETI-DPH method with respect to both the subdomain problem size and the total problem size. For this second-order problem, the lumped and Dirichlet preconditioners deliver similar CPU performances; hence, the lumped preconditioner is preferable since it requires less memory.

Table 2. Performance of the FETI-DPH solver: wheel carrier, undamped, 2^{nd}-order problem; fixed subdomain problem size; $N_\theta = 2$ (+ the three translational rigid body modes); $N_p = 12$

Frequency	Shift (σ^2)	Mesh size	N_s	N_{itr} Lumped	CPU Lumped	N_{itr} Dirichlet	CPU Dirichlet
5×10^5 Hz	9.8e+12	504,375 dof	250	63	64 s.	45	60 s.
		1,317,123 dof	600	70	207 s.	53	206 s.
		2,091,495 dof	950	60	364 s.	45	358 s.
2×10^6 Hz	1.6e+14	504,375 dof	250	137	123 s.	105	119 s.
		1,317,123 dof	600	174	483 s.	140	491 s.
		2,091,495 dof	950	151	901 s.	118	887 s.

To illustrate the performance of the FETI-DPH solver for problems of the form given in (2), the wheel carrier is next assumed to have a Rayleigh damping. The mesh with $N_{dof} = 1,317,123$ is considered, the number of subdomains is set to $N_s = 600$, the shift is set to $\sigma^2 = 10^5$ Hz, the number of wave directions is set to $N_\theta = 2$, the three translational rigid body modes are included in the construction of the augmentation matrix $\mathbf{Q}_b$, and the

number of processors is set to $N_p = 16$. For these parameters, the performance results of FETI-DPH equipped with the lumped preconditioner are reported in Table 3 for the undamped case ($\xi = 0$), and for realistic damping scenarios ($\xi = 1\%$, $\xi = 2\%$, and $\xi = 5\%$). These results suggest that the intrinsic performance of FETI-DPH improves with the amount of damping. For the undamped case, FETI-DPH operates in the real domain. This explains why in that case, each iteration is 2.7 times faster than in the damped case where FETI-DPH operates in the complex plane.

Table 3. Performance of the FETI-DPH solver: wheel carrier, damped, 2^{nd}-order problem; $N_{dof} = 1,317,123$; $N_s = 600$; $\sigma^2 = 10^5$ Hz; lumped preconditioner; $N_\theta = 2$ (+ the three translational rigid body modes); $N_p = 16$

ξ	c_K	c_M	N_{itr}	CPU
0%	0	0	62	182 s.
1%	3.42e-6	17.9	51	403 s.
2%	6.85e-6	35.8	49	394 s.
5%	1.71e-5	89.5	48	384 s.

Next, attention is directed to the undamped alloy wheel problem to investigate the performance for a fourth-order shell problem of the FETI-DPH solver equipped with the Dirichlet preconditioner. Two different frequencies, 5 KHz and 20 KHz, are considered: the upper value of the shift σ^2 arises, for example, when exciting the considered alloy wheel by a frequency that is higher than its $400-th$ natural frequency, or shifting around that frequency during the solution of an eigenvalue problem. The number of subdomains is varied between $N_s = 100$ and $N_s = 400$ and the number of processors is fixed to $N_p = 8$. Table 4, where N_{coarse} denotes the total size of the augmented coarse problem, contrasts for each value of N_s the performance of FETI-DP (with PGMRES as a solver) and the best performance of FETI-DPH obtained by varying N_θ. The reported performance results suggest that the FETI-DPH solver is numerically scalable for dynamic shell problems of the form given in (1). They also highlight the superiority of FETI-DPH over FETI-DP which fails to converge in a reasonable iteration count for large values of the shift σ^2.

Acknowledgement. This research was supported by the Sandia National Laboratories under Contract No. 31095. The first author also acknowledges the support by the Sandia National Laboratories under Contract No. 29341, and the second author also acknowledges partial support by the National Science Foundation under Grant No. DMS-0209297. Any opinions, findings, and conclusions or recommendations expressed in this material are those of the authors and do not necessarily reflect the views of the Sandia National Laboratories or the National Science Foundation.

Table 4. FETI-DPH vs. FETI-DP: alloy wheel, undamped, 4^{th}-order problem; $N_{dof} = 936,102$; Dirichlet preconditioner; $N_p = 8$

Frequency	Shift (σ^2)	N_s	N_θ	N_{coarse}	N_{itr}	CPU
5×10^3 Hz	9.8e+8	100	0	3,258	347	534 s.
		100	3	7,275	122	265 s.
		200	0	6,372	236	301 s.
		200	2	11,853	116	200 s.
		400	0	12,129	226	317 s.
		400	2	21,924	123	271 s.
2×10^4 Hz	1.6e+10	100	0	3,258	>400	–
		100	5	9,512	330	680 s.
		200	0	6,372	>400	–
		200	5	17,581	261	564 s.
		400	0	12,129	>400	–
		400	3	27,270	265	706 s.

References

X. C. Cai and O. Widlund. Domain decomposition algorithms for indefinite elliptic problems. *SIAM J. Sci. Statist. Comput.*, 13:243–258, 1992.

C. Farhat, M. Lesoinne, and K. Pierson. A scalable dual-primal domain decomposition method. *Numer. Lin. Alg. Appl.*, 7:687–714, 2000.

C. Farhat, M. Lesoinne, P. LeTallec, K. Pierson, and D. Rixen. FETI-DP: a dual-primal unified FETI method - part I: a faster alternative to the two-level FETI method. *Internat. J. Numer. Meths. Engrg.*, 50:1523–1544, 2001.

C. Farhat. A Lagrange multiplier based divide and conquer finite element algorithm. *J. Comput. Sys. Engrg.*, 2:149–156, 1991.

C. Farhat and F. X. Roux. A method of finite element tearing and interconnecting and its parallel solution algorithm, *Internat. J. Numer. Meths. Engrg.*, 32:1205–1227, 1991.

C. Farhat, J. Mandel and F. X. Roux. Optimal convergence properties of the FETI domain decomposition method. *Comput. Meths. Appl. Mech. Engrg.*, 115:367–388, 1994.

J. Mandel and R. Tezaur, On the convergence of a dual-primal substructuring method. *Numer. Math.*, 88:543–558, 2001.

A. Klawonn, O. B. Widlund and M. Dryja. Dual-primal FETI methods for three-dimensional elliptic problems with heterogeneous coefficients. *SIAM J. Numer. Anal.*, 40:159–179, 2002.

C. Farhat, P. S. Chen, F. Risler and F. X. Roux. A unified framework for accelerating the convergence of iterative substructuring methods with Lagrange multipliers. *Internat. J. Numer. Meths. Engrg.*, 42:257–288, 1998.

D. Rixen and C. Farhat. A simple and efficient extension of a class of substructure based preconditioners to heterogeneous structural mechanics problems. *Internat. J. Numer. Meths. Engrg.*, 44:489–516, 1999.

C. Farhat, A. Macedo and M. Lesoinne. A two-level domain decomposition method for the iterative solution of high frequency exterior Helmholtz problems. *Numer.Math.*, 85:283–308, 2000.

A. Klawonn. *Preconditioners for Indefinite Problems.* Ph. D. Thesis, Westfalische, Wilhelms-Universitat, Munster, 1995.

Hybrid Schwarz-Multigrid Methods for the Spectral Element Method: Extensions to Navier-Stokes

Paul F. Fischer[1] and James W. Lottes[2]

[1] Argonne National Laboratory, Mathematics and Computer Science Division (http://www.mcs.anl.gov/~fischer/)
[2] University of Illinois, Dept. of Theoretical and Applied Mechanics

Summary. The performance of multigrid methods for the standard Poisson problem and for the consistent Poisson problem arising in spectral element discretizations of the Navier-Stokes equations is investigated. It is demonstrated that overlapping additive Schwarz methods are effective smoothers, provided that the solution in the overlap region is weighted by the inverse counting matrix. It is also shown that spectral element based smoothers are superior to those based upon finite element discretizations. Results for several large 3D Navier-Stokes applications are presented.

1 Introduction

The spectral element method (SEM) is a high-order weighted residual technique that combines the geometric flexibility of finite elements with the rapid convergence properties and tensor-product efficiencies of global spectral methods. Globally, elements are coupled in an unstructured framework with interelement coupling enforced through standard matching of nodal interface values. Locally, functions are represented as tensor products of stable Nth-order Lagrangian interpolants based on Gauss-Lobatto (GL) or Gauss (G) quadrature points. For problems having smooth solutions, such as the incompressible Navier-Stokes equations, the SEM converges exponentially fast with the local approximation order N. Because of its minimal numerical dissipation and dispersion, the SEM is particularly well suited for the simulation of flows at transitional Reynolds numbers, where physical dissipation is small and turbulence-model dissipation is absent.

The two-level hierarchy of the spectral element discretization provides a natural route to domain decomposition with several benefits. The loose C^0 interelement coupling implies that the stencil depth does not increase with approximation order, so that interprocessor communication is minimal. The local tensor-product structure allows matrix-vector products to be recast as cache-efficient *matrix-matrix* products and also allows local subdomain problems to

be solved efficiently with fast tensor-product solvers. Finally, the high-order polynomial expansions provide a readily available sequence of nested grids (obtained through successive reductions in polynomial degree) for use in multilevel solvers.

This paper presents recent developments in spectral element multigrid (SEMG) methods. Our point of departure is the original work of Rønquist and Patera [1987] and Maday and Muñoz [1988], who developed variational SEMG for the two-dimensional Poisson problem using intra-element prolongation/restriction operators coupled with Jacobi smoothing. The high-aspect-ratio cells present in the tensor-product GL grid are a well-known source of difficulty in spectral multigrid methods and have drawn much attention over the past decade. We have developed multigrid smoothers in Lottes and Fischer [2004] based on the overlapping additive Schwarz method of Dryja and Widlund [1987] and Fischer et al. [2000]. We bypass the high-aspect-ratio cell difficulty by solving the local problems directly using fast tensor-product solvers; this approach ensures that the smoother cost does not exceed the cost of residual evaluation. Here, we extend our SEMG approach from the two-dimensional Laplacian to the more difficult consistent Poisson operator that governs the pressure in the mixed $\mathbb{P}_N$– $\mathbb{P}_{N-2}$ spectral element formulation of Maday and Patera [1989].

In the next section, we introduce the SE discretization for a model Poisson problem. The basic elements of our multilevel iterative procedures are presented in Section 3, along with results for the Poisson problem. Extensions to unsteady Navier-Stokes applications are described in Section 4.

2 Discretization of the Poisson Problem

The spectral element discretization of the Poisson problem in $\mathbb{R}^d$ is based on the weighted residual formulation: *Find* $u \in X_N$ *such that*

$$(\nabla v, \nabla u)_{GL} = (v, f)_{GL} \qquad \forall v \in X_N. \tag{1}$$

The inner product $(.,.)_{GL}$ refers to the Gauss-Lobatto-Legendre (GL) quadrature associated with the space $X_N := [Z_N \cap H_0^1(\Omega)]$, where $Z_N := \{v \in L^2(\Omega) | v_{|\Omega^e} \in \mathbb{P}_N(\Omega^e)\}$. Here, L^2 is the space of square integrable functions on Ω; H_0^1 is the space of functions in L^2 that vanish on the boundary and whose first derivative is also in L^2; and $\mathbb{P}_N(\Omega^e)$ is the space of functions on Ω^e whose image is a tensor-product polynomial of degree $\leq N$ in the reference domain, $\widehat{\Omega} := [-1, 1]^d$. For $d = 2$, a typical element in X_N is written

$$u(\mathbf{x}^e(r, s))|_{\Omega^e} = \sum_{i=0}^{N} \sum_{j=0}^{N} u_{ij}^e h_i^N(r) h_j^N(s)\,, \tag{2}$$

where u_{ij}^e is the nodal basis coefficient; $h_i^N \in \mathbb{P}_N$ is the Lagrange polynomial satisfying $h_i^N(\xi_j) = \delta_{ij}$, where ξ_j, $j = 0, \ldots, N$ are the the GL quadrature

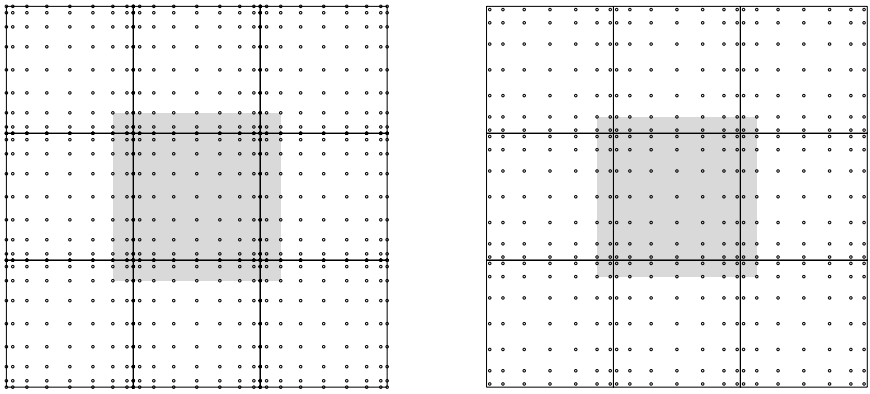

Fig. 1. Spectral element configuration ($E = 9$, $N = 8$) showing Lagrange interpolation points for functions in X^N (left) and Y^N (right). The shaded regions illustrate the "minimal overlap" domain extension for the overlapping Schwarz smoothers

points (the zeros of $(1-\xi^2)L'_N(\xi)$, where L_N is the Legendre polynomial of degree N) and δ_{ij} is the Kronecker delta function; and $\mathbf{x}^e(r,s)$ is the coordinate mapping from $\widehat{\Omega}$ to Ω^e. We assume $\Omega = \cup_{e=1}^{E}\Omega^e$ and that the intersection of two subdomains (spectral elements) is an entire edge, a single vertex, or void. Function continuity ($u \in H^1$) is enforced by ensuring that nodal values on element boundaries coincide with those on adjacent elements. Figure 1 illustrates a spectral element decomposition of the square using $E = 9$ elements. The Gauss-Lobatto-based mesh on the left shows the nodal distribution for X_N. The Gauss-based mesh on the right is used for functions in Y_N, which will be introduced in the context of the Stokes discretization in Section 4.

Computational Preliminaries. Because we employ iterative solvers, we need an efficient procedure for evaluating matrix-vector products associated with the bilinear forms in (1). As noted by Orszag [1980], tensor-product bases play a key role in this respect, particularly for large N (i.e., $N \geq 8$). Here, we introduce several points that are central to our element-based solution strategy.

As with standard finite element methods, we assume availability of both local element-based and global mesh-based node numberings, with the local-to-global map given by $q(i_1,\ldots,i_d,e) \in \{1,\ldots,\bar{n}\}$, for $i_k \in \{0,\ldots,N\}$, $k \in \{1,\ldots,d\}$, and $e \in \{1,\ldots,E\}$, where $\bar{n}$ is the number of distinct global nodes. Let Q^T be the $\bar{n}\times E(N+1)^d$ matrix with columns $\underline{\hat{e}}_{q(i_1,\ldots,i_d,e)}$, where $\underline{\hat{e}}_q$ denotes the qth column of the $\bar{n}\times\bar{n}$ identity matrix. Then the matrix-vector product $\underline{u}_L = Q\underline{u}$ represents a global-to-local mapping for any function $u(\mathbf{x}) \in X^N$, and the bilinear form on the left of (1) can be written

$$(\nabla v, \nabla u) = \underline{v}^T Q^T A_L Q \underline{u}, \tag{3}$$

where A_L=block-diag$(A^e)_{e=1}^E$ is the unassembled stiffness matrix comprising the local stiffness matrices, A^e, and $Q^T$and Q correspond to respective gather and scatter operations. In practice the global stiffness matrix, $A := Q^T A_L Q$, is never formed. One simply effects the *action* of A by applying each matrix to a vector through appropriate subroutine calls.

In the SEM, computational efficiency dictates that *local* stiffness matrices should also be applied in matrix-free form. The local contributions to (3) are

$$(\nabla v, \nabla u)^e_{GL} = (\underline{v}^e)^T A^e \underline{u}^e = (\underline{v}^e)^T \begin{pmatrix} D_1 \\ D_2 \end{pmatrix}^T \begin{pmatrix} G^e_{11} & G^e_{12} \\ G^e_{12} & G^e_{22} \end{pmatrix} \begin{pmatrix} D_1 \\ D_2 \end{pmatrix} \underline{u}^e, \qquad (4)$$

with respective geometric factors and derivative operators,

$$G^e_{ij} := \left(\widehat{B} \otimes \widehat{B}\right) \left[\sum_{k=1}^{d} \frac{\partial r_i}{\partial x_k} \frac{\partial r_j}{\partial x_k}\right]^e J^e, \quad D_1 := (I \otimes \widehat{D}), \quad D_2 := (\widehat{D} \otimes I). \quad (5)$$

Here, $\underline{v}^e$ and $\underline{u}^e$ are vectors containing the lexicographically ordered nodal basis coefficients $\{v^e_{ij}\}$ and $\{u^e_{ij}\}$, respectively; $\widehat{B}$=diag$(\rho_k)_{k=0}^N$ is the one-dimensional mass matrix composed of the GL quadrature weights; and $\widehat{D}$ is the one-dimensional derivative matrix with entries

$$\widehat{D}_{ij} = \left.\frac{dh_j}{dr}\right|_{\xi_i}, \qquad i,j \in \{0,\ldots,N\}^2.$$

The Jacobian, J^e, and metric terms (in brackets in (5)) are evaluated pointwise at each GL quadrature point, (ξ_p, ξ_q), so that each of the composite geometric matrices, G^e_{ij}, is diagonal.

The presence of the cross terms, G^e_{12}, implies that A^e is full and requires storage of $(N+1)^4$ nonzeros for *each* spectral element if explicitly formed. In the spectral element method, this excessive storage and work overhead is avoided by retaining the factored form (5), which requires (to leading order) storage of only $3E(N+1)^2$ nonzeros and work of $\approx 8E(N+1)^3$ per matrix-vector product. The savings is more significant in 3D, where the respective storage and work complexities are $6E(N+1)^3$ and $\approx 12E(N+1)^4$ for the factored form, versus $O(EN^6)$ if A is explicitly formed. Moreover, the leading order work terms for the factored form can be cast as efficient matrix-matrix products, as discussed in detail by Deville et al. [2002]. These complexity savings can be extended to all system matrices and are the basis for efficient realizations of high-order weighted residual techniques.

If Ω^e is a regular parallelepiped, the local stiffness matrix simplifies to a separable form. For example, for an $L^e_x \times L^e_y$ rectangle, one would have

$$A^e = \frac{L^e_y}{L^e_x} \widehat{B} \otimes \widehat{A} + \frac{L^e_y}{L^e_x} \widehat{A} \otimes \widehat{B}, \qquad \widehat{A} := \widehat{D}^T \widehat{B} \widehat{D}. \qquad (6)$$

This form has a readily computable (pseudo-) inverse given by the fast diagonalization method (FDM) of Lynch et al. [1964],

$$A_e^{-1} \;=\; (S \otimes S)\left[\frac{L_y^e}{L_x^e} I \otimes \Lambda + \frac{L_y^e}{L_x^e} \Lambda \otimes I\right]^{-1} (S^T \otimes S^T), \tag{7}$$

where S is the matrix of eigenvectors and Λ the matrix of eigenvalues satisfying $\widehat{A}S = \widehat{B}S\Lambda$ and $S^T\widehat{B}S = I$. The bracketed term in (7) is diagonal, and its pseudo-inverse is computed by inverting nonzero elements and retaining zeros elsewhere. For arbitrarily deformed elements, the discrete Laplacian cannot be expressed in the tensor-product form (6), and the FDM cannot be used. For the purposes of a preconditioner, however, it suffices to apply the FDM to a regular parallelepiped of equivalent size, as demonstrated in Couzy [1995] and Fischer et al. [2000]. Similar strategies for the case of nonconstant coefficients are discussed by Shen [1996].

3 Multilevel Solvers

We are interested in methods for solving the global system $A\underline{u} = \underline{g}$. To introduce notation, we consider the two-level multigrid sweep.

Procedure Two-Level: (8)

i) $\underline{u}^{k+1} = \underline{u}^k + \sigma M(\underline{g} - A\underline{u}^k), \qquad k = 0, \ldots, m_d - 1$

ii) $\underline{r} = \underline{g} - A\underline{u}^{m_d}$

iii) $\tilde{\underline{e}} = \sigma_C P A_C^{-1} P^T \underline{r}$

iv) $\tilde{\underline{u}}^0 = \underline{u}^{m_d} + \tilde{\underline{e}}$

v) $\tilde{\underline{u}}^{k+1} = \tilde{\underline{u}}^k + \sigma M(\underline{g} - A\tilde{\underline{u}}^k), \qquad k = 0, \ldots, m_u - 1$

vi) If $||A\tilde{\underline{u}}^{m_u} - \underline{g}|| < \text{tol}$, set $\underline{u} := \tilde{\underline{u}}^{m_u}$, *quit.*
Else, $\underline{u}^0 := \tilde{\underline{u}}^{m_u}$, go to (*i*).

Here M is the smoother, σ and σ_C are relaxation parameters, and m_d and m_u are the number of smoothing steps on the downward and upward legs of the cycle, respectively. Steps (*i*) and (*v*) are designed to eliminate high-frequency error components that cannot be represented on the coarse grid. The idea is that the error after (*ii*), $\underline{e} := A^{-1}\underline{r}$, should be well approximated by $\tilde{\underline{e}}$, which lies in the coarse-grid space represented by the columns of P. The coarse-grid problem, A_C^{-1}, is solved directly, if A_C is sufficiently sparse, or approximated by recursively applying the two-level procedure to the A_C system, giving rise to the multigrid "V" cycle. The prolongation matrix P interpolates from the coarse space to the fine nodes using the local tensor-product basis functions for the coarse space.

If the two-level procedure is used as a preconditioner, we take $\underline{u}^0 = 0$, $m_d = 1$, and $m_u = 0$, and the procedure simplifies to the following.

Procedure Preconditioner: (9)

$$
\begin{aligned}
&i)\ \ \underline{u}^1 = \sigma M \underline{g},\\
&ii)\ \ \underline{r} = \underline{g} - A\underline{u}^1\\
&iii)\ \ \tilde{\underline{e}} = \sigma_C P A_C^{-1} P^T \underline{r}\\
&iv)\ \ \underline{u} = \underline{u}^1 + \tilde{\underline{e}},\ \text{return.}
\end{aligned}
$$

The preconditioner can be viewed either as an application of the multigrid V-cycle or as a two-level multiplicative Schwarz method (Smith et al. [1996]). By simply replacing (ii) with $\underline{r} = \underline{g}$, we obtain a two-level additive Schwarz method, which has the advantage of avoiding an additional multiplication by A. This savings is important in the Navier-Stokes applications that we consider in Section 4.

Smoothers for the Poisson Problem. Here, we review the SEMG smoothing strategies considered for the Poisson problem in Lottes and Fischer [2004]. Our original intent was to base the smoother, M, on the additive overlapping Schwarz method of Dryja and Widlund [1987], with local subdomain problems discretized by finite elements (FEs) having nodes coincident with the GL nodes, as considered by Casarin [1997], Fischer [1997], and Pahl [1993]. By using the fast diagonalization method to solve the local problems, however, we are freed from the constraint of using FE-based preconditioners because the cost depends only on the use of tensor-product forms and not on the sparsity of the originating operator. Hence, we are able to consider subdomain problems derived as restrictions of the originating spectral element matrix, A, as first suggested by Casarin [1997].

The use of Schwarz-based smoothing, which is arguably more expensive than traditional smoothers, is motivated by several factors. First, it is not practical to apply Gauss-Seidel smoothing in the SEM because the matrix entries are not available (see (4)). The alternative of pointwise-Jacobi smoothing was shown by Rønquist [1988] and Maday et al. [1992] not to scale for $d > 1$. Specifically, the authors demonstrated a convergence factor of $\rho = 0.75$ for $d = 1$, but only $\rho = 1 - c/N \log N$ for $d = 2$. Second, while one can exploit the SE-FE spectral equivalence established by Orszag [1980] to ostensibly convert the SE problem into a FE problem and then apply traditional multigrid, the FE problem inherits the difficulties of its SE counterpart, namely, the high-aspect ratio cells that arise from the tensor-product of the one-dimensional Gauss-Lobatto grids. Moreover, even if the GL-based FE problem could be solved with low work, the iteration count would still be higher than what is observed for the Schwarz-based approach. Third, to minimize cost, it is reasonable to have a smoother whose cost is on par with that of residual evaluation if it can substantially reduce the iteration count.

We illustrate the problem of high-aspect ratio cells by considering application of the two-level procedure (8) to the model Poisson problem (1) discretized on the unit square with an $8N \times 8N$ array of bilinear finite elements.

Table 1. MG method on FE problem

FE Spacing	No.	Smoother/ Preconditioner	Coarse Space	Iterations, 10^{-11} Reduction			
				$N = 4$	$N = 8$	$N = 12$	$N = 16$
Uniform	a	Jacobi	$N/2$	39	38	38	38
	b	GSRB	$N/2$	9	9	9	9
	c	H Schwarz	$N/2$	40	41	42	42
	d	H Schwarz (W)	$N/2$	7	7	6	6
SE	e	Jacobi	$N/2$	41	84	148	219
	f	GSRB	$N/2$	11	28	46	65
	g	H Schwarz	$N/2$	40	43	47	52
	h	H Schwarz (W)	$N/2$	6	7	7	9

Iteration counts for four different smoothing strategies are shown in Table 1. Jacobi implies M^{-1}:=diag(A); GSRB is a Gauss-Seidel sweep with the nodes ordered into two maximally independent ("red-back") subsets; and H Schwarz and H Schwarz(W) correspond to the hybrid Schwarz-based smoothers introduced below. In all cases, σ is chosen such that the maximum eigenvalue of σMA is unity, and $\sigma_C = 1$. The coarse system is solved directly and is based on the same FE discretization, save that, in each direction, every other nodal point is discarded. The first set of results is for uniformly sized elements of length $1/8N$ on each side. Resolution-independent convergence is obtained for each of the smoothing strategies, with GSRB and H Schwarz(W) being the most competitive. Although H Schwarz(W) has a lower iteration count, GSRB requires less work per iteration, and the two are roughly equal in computational cost. The second set of results is for an $8N\times8N$ array of bilinear elements whose vertices coincide with the GL node spacing associated with an 8×8 array of spectral elements of order N. In this case, the pointwise Jacobi and GSRB smoothers break down as N is increased. Only H Schwarz(W) retains performance comparable to the uniform grid case. We note that line-based relaxation strategies proposed by Shen et al. [2000] and Beuchler [2002] also compensate for the high-aspect-ratio cell difficulty. For the values of N considered here, however, the hybrid Schwarz approach is likely to be faster, at least on cache-based architectures, where the matrix-matrix product-oriented fast-diagonalization method is very effective.

Our hybrid Schwarz strategy is based on a multiplicative combination of an additive Schwarz smoother at the fine scale and a coarse-grid correction. The smoother, originally due to Dryja and Widlund [1987], is written as

$$M := \sum_{e=1}^{E} R_e^T A_e^{-1} R_e. \tag{10}$$

Here, R_e is the standard Boolean restriction matrix that extracts from a global nodal vector those values associated with the *interior* of the extended subdomain $\bar{\Omega}^e$. In all cases, $\bar{\Omega}^e$ is an extension of Ω^e that includes a single row

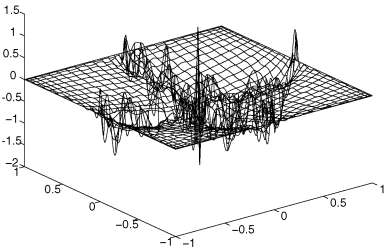

(a) Application of M

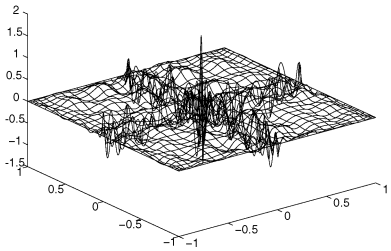

(b) Coarse solver after (a)

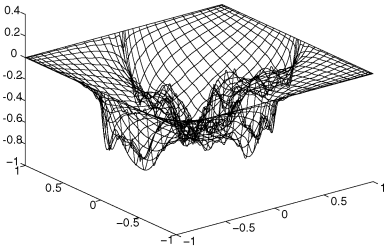

(c) Application of WM

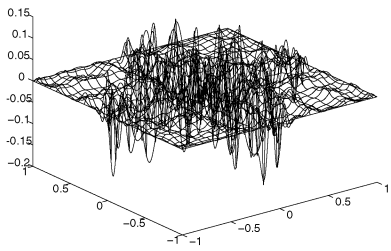

(d) Coarse solver after (c)

Fig. 2. Error plots for the hybrid Schwarz preconditioner and coarse solve, with $N_C = N/2$ and $(E, N) = (4, 16)$, applied to a random initial guess

(or plane, in 3D) of nodal values in each of $2d$ directions. as illustrated in Fig. 1 (left). R_e^T extends by zero the vector of nodal values interior to $\bar{\Omega}^e$ to a full length vector. Multiplication by A_e^{-1} is effected by using the fast diagonalization method similar to (7). In a preprocessing step, one assembles *one-dimensional* stiffness and mass matrices, A_* and B_* ($* = x$, y or z), for each space dimension, $1, \ldots, d$; restricts these to the relevant ranges using a one-dimensional restriction matrix R_*^e; and solves an eigenvalue problem of the form $((R_*^e)^T A_* R_*^e) S_*^e = ((R_*^e)^T B_* R_*^e) S_*^e \Lambda_*^e$ to obtain the requisite eigenpairs (S_*^e, Λ_*^e). Because the spectral elements are compactly supported, the preprocessing step requires knowledge only of the size of the elements on either side of Ω^e, in each of the d directions. For subdomains that are not rectilinear, A_e is based on average lengths in each direction.

We have found it important to weight the solutions in the overlap region by the inverse of the diagonal counting matrix

$$C := \sum_{e=1}^{E} R_e^T R_e. \tag{11}$$

The entries of C enumerate the number of subdomains that share a particular vertex. Setting $W = C^{-1}$ gives rise to the weighted overlapping Schwarz smoother $M_W := WM$. Although convergence theory for the weighted

Schwarz method is yet to be developed, the methodology of Frommer and Szyld [2001] should be applicable to this setting as well. In addition to reducing the maximum eigenvalue of MA (which, by simple counting arguments, is $\max C_{ii}$; see Smith et al. [1996]), multiplication by W significantly improves the smoothing performance of the additive Schwarz step. This latter point is illustrated in Fig. 2, which shows the error when the two-level preconditioner (9) is applied to random right-hand-side vector for a 2×2 array of spectral elements with N=16. Figure 2(a) shows the error after a single application of the additive Schwarz smoother (10), with σ=1. While the solution is smooth in the interior, there is significant undamped error along the interface, particularly at the cross point. As noted by Lottes and Fischer [2004], the error along the interface can be reduced by choosing $\sigma = 1/4$, but the overall error is no longer smooth. In either case, the subsequent coarse-grid correction does not yield a significant error reduction. By contrast, the error after application of M_W, seen in Fig. 2(c), is relatively smooth, and the coarse-grid correction is very effective. Comparing the magnitudes in Figs. 2(b) and 2(d), one sees a tenfold reduction in the error through the introduction of W.

Table 2 presents convergence results for the Poisson problem on the square discretized with an 8×8 array of spectral elements. Case 2(a) shows results for the unweighted additive Schwarz preconditioner using an FE-based smoother. This scheme is the Poisson equivalent to the method developed by Fischer et al. [2000] for the pressure subproblem considered in the next section. For all the other cases, A_e is based on a restriction of A rather than on an FE discretization. Case 2(b) shows that this simple change considerably reduces the iteration count. Enriching the coarse space from $N_C = 1$ to $N/2$ and incorporating the weight matrix W yields further reductions in iteration count and work. (Because of symmetry requirements, W is applied as a pre- and postmultiplication by $W^{1/2}$ for the preconditioned conjugate gradient, PCG, cases). The work shown in the last column of Table 2 is an estimate of the number of equivalent matrix-vector products required to reduce the error by 10^{-11}. Rather than attempting to symmetrize the hybrid Schwarz method (9), we simply switched to GMRES, which allowed W to be applied directly during the summation of the overlapping solutions. Comparison of cases 2(f) and 2(h) underscores the importance of weighting.

4 Extension to Navier-Stokes

Efficient solution of the incompressible Navier-Stokes equations in complex domains depends on the availability of fast solvers for sparse linear systems. For unsteady flows, the pressure operator is the leading contributor to stiffness, as the characteristic propagation speed is infinite. Our pressure solution procedure involves two stages. First, we exploit the fact that we solve similar problems from one step to the next by projecting the current solution onto a subspace of previous solutions to generate a high-quality initial approxima-

Table 2. Iteration count for E=8×8 SE problem

Method	No.	Smoother/ Preconditioner	Coarse Space	Iterations, 10^{-11} Reduction $N=4$	$N=8$	$N=12$	$N=16$	Work $N=16$
PCG	a	A Schwarz (FE)	1	28	35	46	58	116
	b	A Schwarz	1	25	27	35	43	86
	c	A Schwarz	$N/2$	26	26	26	27	81
	d	A Schwarz (W)	1	17	24	33	43	86
	e	A Schwarz (W)	$N/2$	16	21	22	24	72
MG/ GMRES	f	H Schwarz	$N/2$	21	23	24	25	100
	g	H Schwarz (W)	1	14	20	29	36	108
	h	H Schwarz (W)	$N/2$	13	12	12	13	52

tion, as outlined in Fischer [1998]. We then compute the correction to this approximation using a scalable iterative solver. Here, we extend the multigrid methods presented in the preceding sections to computation of the pressure in SE-based simulations of incompressible flows.

To introduce notation, we review the Navier-Stokes discretization presented in detail in Fischer [1997]. The temporal discretization is based on a semi-implicit scheme in which the nonlinear term is treated explicitly and the remaining unsteady Stokes problem is solved implicitly. Our spatial discretization is based on the $\mathbb{P}_N - \mathbb{P}_{N-2}$ spectral element method of Maday and Patera [1989]. Assuming $\mathbf{f}^n$ incorporates all terms explicitly known at time t^n, the $\mathbb{P}_N - \mathbb{P}_{N-2}$ formulation of the Navier-Stokes problem reads: *Find* $(\mathbf{u}^n, p^n) \in X_N \times Y_N$ *such that*

$$\begin{aligned} \frac{1}{Re}(\nabla \mathbf{v}, \nabla \mathbf{u}^n)_{GL} + \frac{1}{\Delta t}(\mathbf{v}, \mathbf{u}^n)_{GL} - (\nabla \cdot \mathbf{v}, p^n)_G &= (\mathbf{v}, \mathbf{f^n})_{GL}, \\ (q, \nabla \cdot \mathbf{u}^n)_G &= 0, \end{aligned} \tag{12}$$

$\forall\, (\mathbf{v}, q) \in X_N \times Y_N$. The inner products $(.,.)_{GL}$ and $(.,.)_G$ refer to the Gauss-Lobatto-Legendre (GL) and Gauss-Legendre (G) quadratures associated with the spaces $X_N := [Z_N \cap H_0^1(\Omega)]^d$ and $Y_N := Z_{N-2}$, respectively, and Z_N is the space introduced in conjunction with (1). The local velocity basis is given, componentwise, by the form (2). The pressure is similar, save that the nodal interpolants are based on the N-1 Gauss points, $\eta_i \in (-1, 1)$, as illustrated in Fig. 1 (right).

Insertion of the SEM bases into (12) yields a discrete Stokes system to be solved at each step:

$$\mathbf{H}\,\underline{\mathbf{u}}^n - \mathbf{D}^T\,\underline{p}^n = \mathbf{B}\,\underline{\mathbf{f}}^n, \;\; \mathbf{D}\,\underline{\mathbf{u}}^n = 0. \tag{13}$$

$\mathbf{H} = \frac{1}{Re}\mathbf{A} + \frac{1}{\Delta t}\mathbf{B}$ is the discrete equivalent of the Helmholtz operator, $(-\frac{1}{Re}\nabla^2 + \frac{1}{\Delta t})$; $-\mathbf{A}$ is the discrete Laplacian; $\mathbf{B}$ is the (diagonal) mass matrix associated with the velocity mesh; $\mathbf{D}$ is the discrete divergence operator, and $\mathbf{f}^n$ accounts for the explicit treatment of the nonlinear terms. Note that

the Galerkin approach implies that the governing system in (13) is symmetric and that the matrices $\mathbf{H}$, $\mathbf{A}$, and $\mathbf{B}$ are all symmetric positive definite. We have used bold capital letters to indicate matrices that interact with vector fields.

The Stokes system (13) is advanced by using the operator splitting approach presented by Maday et al. [1990] and Perot [1993]. One first solves

$$\mathbf{H}\,\underline{\hat{\mathbf{u}}} = \mathbf{B}\,\underline{\mathbf{f}}^n + \mathbf{D}^T\,\underline{p}^{n-1}, \tag{14}$$

which is followed by a pressure correction step

$$E\,\delta\underline{p}^n = -\frac{1}{\Delta t}\mathbf{D}\underline{\hat{\mathbf{u}}}, \qquad \underline{\mathbf{u}}^n = \underline{\hat{\mathbf{u}}} + \Delta t\mathbf{B}^{-1}\mathbf{D}^T\delta\underline{p}^n, \qquad \underline{p}^n = \underline{p}^{n-1} + \delta\underline{p}^n, \tag{15}$$

where $E := \mathbf{D}\mathbf{B}^{-1}\mathbf{D}^T$ is the Stokes Schur complement governing the pressure in the absence of the viscous term.

E is the consistent Poisson operator for the pressure and is spectrally equivalent to A. Through a series of tests that will be reported elsewhere, we have found the following to be an effective multilevel strategy for solving E. We employ (9) to precondition GMRES with a weighted additive Schwarz smoother. The local problems are based on $E_e := \tilde{R}_e E \tilde{R}_e^T$, where the subdomains defined by the restriction matrices $\tilde{R}_e$ correspond to the minimal-overlap extension illustrated in Fig. 1 (right). The coarse-grid problem, A_C, is based on A with $N_C = N/2$ (typically), which was found not only to be cheaper but also better at removing errors along the element interfaces. At all intermediate levels, A_C^{-1} is approximated with a single V-cycle (8).

The local problems are solved using the fast diagonalization method, which requires that E_e (and therefore E) be separable. In two dimensions, we need to cast E in the form

$$E \;=\; J_y \otimes E_x \;+\; E_y \otimes J_x. \tag{16}$$

For simplicity, we assume that we have a single element with $\Omega = \widehat{\Omega}$ and ignore the details of boundary conditions. From the definition of E, we have

$$E \;=\; D_x B^{-1} D_x^T \;+\; D_y B^{-1} D_y^T. \tag{17}$$

The divergence and inverse mass matrices have the tensor-product forms

$$D_x = (\widetilde{B} \otimes \widetilde{B})(\widetilde{J} \otimes \widetilde{D}), \quad D_y = (\widetilde{B} \otimes \widetilde{B})(\widetilde{D} \otimes \widetilde{J}), \quad B^{-1} = (\widehat{B}^{-1} \otimes \widehat{B}^{-1}) \tag{18}$$

Here, $\widetilde{B}$=diag$(\tilde{\rho}_i)_{i=1}^{N-1}$ consists of the Gauss-Legendre quadrature weights, and $\widetilde{J}$ and $\widetilde{D}$ are respective interpolation and derivative matrices mapping from the GL points to the G points,

$$\widetilde{J}_{ij} = h_j^N(\eta_i), \qquad\qquad \widetilde{D}_{ij} = \left.\frac{dh_j^N}{dr}\right|_{r=\eta_i}. \tag{19}$$

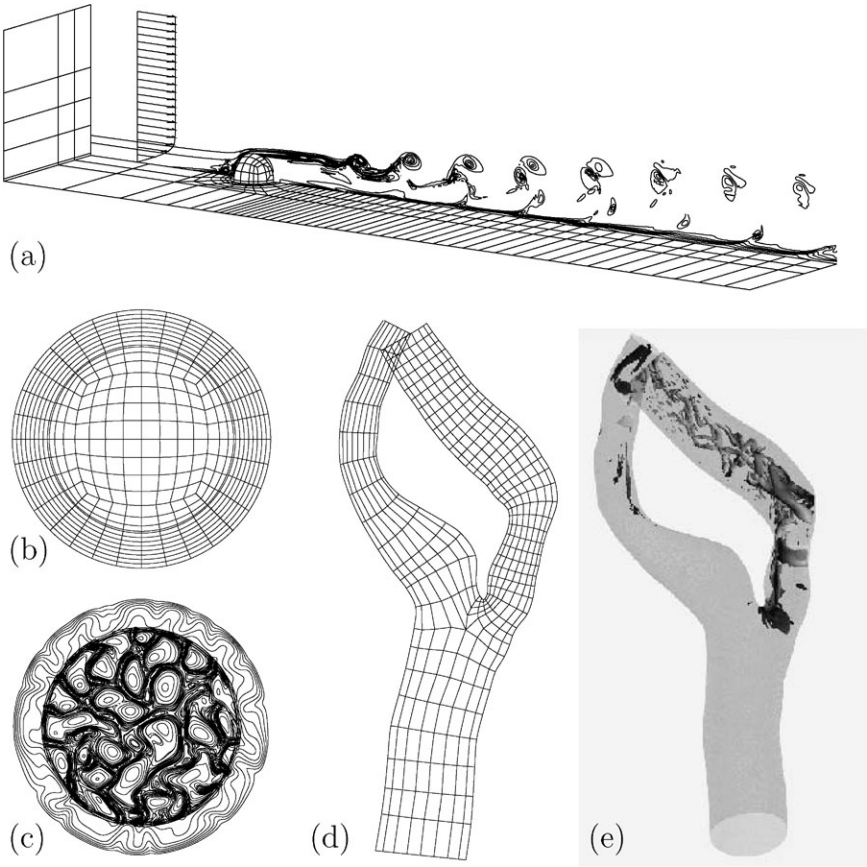

Fig. 3. SE Navier-Stokes examples: (a) $E = 1021$ mesh, inlet profile, and vorticity contours for roughness element; (b) $E = 1536$ mesh and (c) temperature contours for buoyancy driven convection; (d) $E = 2544$ mesh and (e) coherent structures for flow in a diseased carotid artery

Inserting (18) into (17) yields the desired form (16) with

$$J_x = J_y = \widetilde{B}\widetilde{J}\widehat{B}^{-1}\widetilde{J}^T\widetilde{B}^T, \qquad E_x = E_y = \widetilde{B}\widetilde{D}\widehat{B}^{-1}\widetilde{D}^T\widetilde{B}^T. \tag{20}$$

The extension to multiple elements follows by recognizing that the gather-scatter operator used to assemble the local matrices can be written as $Q = Q_y \otimes Q_x$ for a tensor-product array of elements. Following our element-centric solution strategy, we thus generate E_e by viewing Ω^e as being embedded in a 3^d array of rectilinear elements of known dimensions. Unlike A_e, the entries of E_e are also influenced by the "neighbors of neighbors." This influence, however, is small and is neglected.

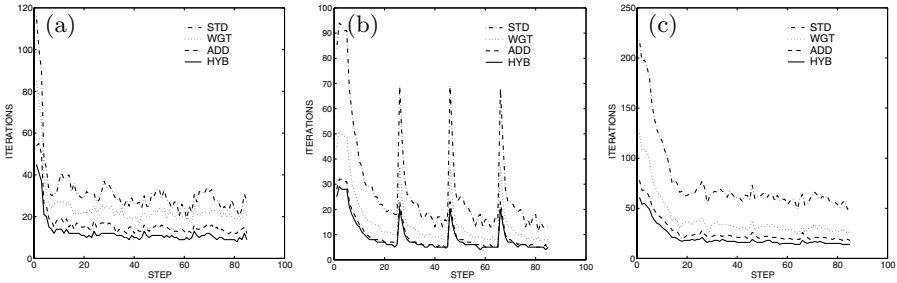

Fig. 4. Iteration histories for FE-based two-level (STD), weighted SE-based two-level (WGT), additive multilevel (ADD), and multiplicative multilevel (HYB) schemes for spectral elements simulations of order N=9: (a) hairpin vortex, E=1021; (b) hemispherical convection, E=1536; and (c) carotid artery simulation, E=2544

Navier-Stokes Results. We turn now to application of spectral element multigrid (SEMG) to the simulation of unsteady incompressible flows. In numerous 2D and 3D Navier-Stokes test problems, we have found the additive variant of the procedure outlined in the preceding section to be roughly two to three times faster than the two-level additive Schwarz method developed in Fischer et al. [2000]. A sample of these results is presented below.

We consider the three test cases shown in Fig. 3. The first case, Fig. 3(a), is boundary-layer flow past a hemispherical roughness element at Reynolds number Re=1000 (based on roughness height). The flow generates a pre-transitional chain of hairpin vortices evidenced by the spanwise vorticity contours shown in the symmetry plane. The second example, Fig. 3(b)-(c), is buoyancy-driven convection in a rotating hemispherical shell having inner radius 2.402 and outer radius 3.3. The Rayleigh number (based on shell thickness) is Ra=20,000 and the Taylor number is Ta=160,000. The third case, Fig. 3(d)-(e), simulates transitional flow in a diseased carotid artery. The severe stenosis in the internal (right) branch results in high flow velocities and, ultimately, transition to turbulence. Figure 3(e) shows the coherent structures that arise just before peak systole.

Figure 4 shows the pressure iteration history for the first 85 timesteps of the three examples, using the initial conditions of Fig. 3. For all cases, N=9 and the coarse problem is based on linear elements whose vertices are derived from an oct-refinement of the SE mesh. Four methods are considered: STD refers to the two-level additive Schwarz method of Fischer et al. [2000]; WGT is the same as STD, save that E_e is based on a restriction of E, rather than an FE-based discretization of the Poisson problem, and that the weight matrix W is included; ADD is the same as WGT, save that three levels are employed, with N_{mid}=5; HYB is the same as ADD, save that the multiplicative variant of (9) is used. PCG is used for STD and WGT, whereas GMRES is used for ADD and HYB. Although HYB requires fewer iterations, ADD is the fastest method

Table 3. ADD Avg. Iteration Count for Navier-Stokes Examples

Problem	N=5	N=7	N=9	N=11	N=13	N=15	N=17
Hairpin Vortex	9.8	11.1	15.1	17.5	20.4	23.5	26.1
Spherical Conv.	8.2	7.8	8.3	8.9	9.9	10.9	11.6
Carotid Artery	18.5	20.6	23.7	26.0	29.3	32.5	36.0
Carotid (WGT)	16.5	22.2	30.0	39.5	48.4	59.4	65.8

because it requires only one product in E per iteration. The prominent spikes in Fig. 4(b) result from resetting the projection basis set (Fischer [1998]).

The scalability of the three-level ADD method is illustrated in Table 3, which shows the average iteration count over the last 20 steps for varying N with $N_{\text{mid}}=N/2$. Order-independence is not assured in complex domains, particularly if the mesh contains high aspect-ratio elements (Fischer [1997]). The performance of ADD is nonetheless quite reasonable when one considers that the number of pressure nodes varies by a factor of 64 in moving from $N = 5$ to 17. For purposes of comparison, results for the WGT method are shown for the carotid. The additional level of ADD clearly reduces order dependence.

Acknowledgement. This work was supported by the Mathematical, Information, and Computational Sciences Division subprogram of the Office of Advanced Scientific Computing Research, Office of Science, U.S. Department of Energy, under Contract W-31-109-Eng-38.

References

S. Beuchler. Multigrid solver for the inner problem in domain decomposition methods for p-fem. *SIAM J. Numer. Anal.*, 40:928–944, 2002.

M. A. Casarin. Quasi-optimal Schwarz methods for the conforming spectral element discretization. *SIAM J. Numer. Anal.*, 34:2482–2502, 1997.

W. Couzy. *Spectral Element Discretization of the Unsteady Navier-Stokes Equations and its Iterative Solution on Parallel Computers.* PhD thesis, Swiss Federal Institute of Technology-Lausanne, 1995. Thesis nr. 1380.

M. O. Deville, P. F. Fischer, and E. H. Mund. *High-order methods for incompressible fluid flow.* Cambridge University Press, Cambridge, 2002.

M. Dryja and O. B. Widlund. An additive variant of the Schwarz alternating method for the case of many subregions. Technical Report TR 339, Courant Inst., NYU, 1987. Dept. Comp. Sci.

P. F. Fischer. An overlapping Schwarz method for spectral element solution of the incompressible Navier-Stokes equations. *J. Comput. Phys.*, 133:84–101, 1997.

P. F. Fischer. Projection techniques for iterative solution of $Ax = b$ with successive right-hand sides. *Comput. Methods Appl. Mech. Engrg.*, 163: 193–204, 1998.

P. F. Fischer, N. I. Miller, and H. M. Tufo. An overlapping Schwarz method for spectral element simulation of three-dimensional incompressible flows. In P. Bjørstad and M. Luskin, editors, *Parallel Solution of Partial Differential Equations*, pages 158–180, Berlin, 2000. Springer.

A. Frommer and D. B. Szyld. An algebraic convergence theory for restricted additive Schwarz methods using weighted max norms. *SIAM Journal on Numerical Analysis*, 39:463–479, 2001.

J. W. Lottes and P. F. Fischer. Hybrid multigrid/Schwarz algorithms for the spectral element method. *J. Sci. Comput.*, (to appear), 2004.

R. E. Lynch, J. R. Rice, and D. H. Thomas. Direct solution of partial difference equations by tensor product methods. *Numer. Math.*, 6:185–199, 1964.

Y. Maday and R. Muñoz. Spectral element multigrid: Numerical analysis. *J. Sci. Comput.*, 3:323–354, 1988.

Y. Maday, R. Muñoz, A. T. Patera, and E. M. Rønquist. Spectral element multigrid methods. In P. de Groen and R. Beauwens, editors, *Proc. of the IMACS Int. Symposium on Iterative Methods in Linear Algebra, Brussels, 1991*, pages 191–201, Amsterdam, 1992. Elsevier.

Y. Maday and A. T. Patera. Spectral element methods for the Navier-Stokes equations. In A. K. Noor and J. T. Oden, editors, *State-of-the-Art Surveys in Computational Mechanics*, pages 71–143. ASME, New York, 1989.

Y. Maday, A. T. Patera, and E. M. Rønquist. An operator-integration-factor splitting method for time-dependent problems: Application to incompressible fluid flow. *J. Sci. Comput.*, 5:263–292, 1990.

S. A. Orszag. Spectral methods for problems in complex geometry. *J. Comput. Phys.*, 37:70–92, 1980.

S. S. Pahl. Schwarz type domain decomposition methods for spectral element discretizations. Master's thesis, Univ. of Witwatersrand, Johannesburg, South Africa, 1993. Dept. of Computational and Applied Math.

J. B. Perot. An analysis of the fractional step method. *J. Comp. Phys.*, 108: 51–58, 1993.

E. Rønquist. *Optimal Spectral Element Methods for the Unsteady Three-Dimensional Incompressible Navier-Stokes Equations*. PhD thesis, Massachusetts Institute of Technology, 1988. Cambridge, MA.

E. M. Rønquist and A. T. Patera. Spectral element multigrid, I:. Formulation and numerical results. *J. Sci. Comput.*, 2:389–406, 1987.

J. E. Shen. Efficient Chebyshev-Legendre Galerkin methods for elliptic problems. In A. V. Ilin and L. R. Scott, editors, *Third Int. Conference on Spectral and High Order Methods*, pages 233–239. Houston Journal of Mathematics, 1996.

J. E. Shen, F. Wang, and J. Xu. A finite element multigrid preconditioner for Chebyshev-collocation methods. *Appl. Numer. Math.*, 33:471–477, 2000.

B. Smith, P. Bjørstad, and W. Gropp. *Domain Decomposition: Parallel Multilevel Methods for Elliptic PDEs*. Cambridge University Press, Cambridge, 1996.

Numerical Approximation of Dirichlet-to-Neumann Mapping and its Application to Voice Generation Problem

Takashi Kako and Kentarou Touda

The University of Electro-Communications, Department of Computer Science
(http://www.im.uec.ac.jp/~kako/EngIntro.html)

Summary. In this paper, we treat the numerical method for the Helmholtz equation in unbounded region with simple cylindrical or spherical shape outside some bounded region and apply the method to voice generation problem. The numerical method for the Helmholtz equation in unbounded region is based on the domain decomposition technique to divide the region into a bounded region and the rest unbounded one. We then treat the approximation of the artificial boundary condition given through the DtN mapping on the artificial boundary. We apply the finite element approximation to discretize the problem. In applying the method to the voice generation problem, it is essential to compute the frequency response function or the formant curve. We give variational formulas for the resolvent poles with respect to the variation of vocal tract boundary which determine the peaks of frequency response function known as formants, and we propose the use of variational formulas to design the location of formants.

1 Numerical Method for Exterior Helmholtz Problem

1.1 Formulation of Exterior Helmholtz Problem

We consider the following 2-dimensional exterior Helmholtz equation with unknown function u as the mathematical model for the time stationary problem of outgoing or radiation sound wave propagation in unbounded region outside an obstacle:

$$-\Delta u - k^2 u = 0 \qquad \text{in } \Omega = R^2 \backslash \mathcal{O}, \tag{1}$$

$$\frac{\partial u}{\partial n} = g \qquad \text{on } \partial\Omega, \tag{2}$$

$$\lim_{r\to\infty} \sqrt{r}\left(\frac{\partial u}{\partial r} - \mathbf{i}ku\right) = 0, \qquad \mathbf{i} = \sqrt{-1}, \tag{3}$$

where Ω is the interior of the complement of a bounded obstacle $\mathcal{O}$ in R^2 with smooth boundary $\partial\Omega$ on which the Neumann boundary condition (2) is

imposed with an inhomogeneous data g. A real constant k is called a wave number and the condition (3) is the Sommerfeld radiation condition at infinity which excludes any unphysical incoming wave. In the case with tubular cylindrical outside region, a similar formulation is possible with necessary modification of boundary condition and radiation condition (see Section 2.2).

Related to this problem in unbounded region, we introduce a circular artificial boundary Γ_R with radius R and decompose the original domain into two sub-domains. We then consider the boundary value problem in the part of bounded sub-domain given as

$$-\Delta u - k^2 u = 0 \qquad \text{in } \Omega_R \equiv \Omega \cap B_R, \tag{4}$$

$$\frac{\partial u}{\partial n} = g \qquad \text{on } \partial\Omega, \tag{5}$$

$$\frac{\partial u}{\partial r} = Mu \qquad \text{on } \Gamma_R, \tag{6}$$

where $B_R \supset\supset \mathcal{O}$ is a circular domain with radius R bounded by an artificial circular boundary Γ_R: $B_R = \{(x,y) \mid r \equiv \sqrt{x^2+y^2} < R\}$, and M is a differential or pseudo-differential operator which we construct as a function of the operator $\partial^2/\partial\theta^2$ of angular variable θ in order to make the problem exactly or approximately equivalent to the original problem.

The exact solution $u(r,\theta)$ for (1)-(3) in B_R^c is given by the following formula with the Hankel function of the first kind of order n which we will denote in this paper by $H^{(1)}(\cdot\ ;\ n)(= H_n^{(1)}(\cdot))$:

$$u(r,\theta) = \frac{1}{2\pi} \sum_{n=-\infty}^{\infty} \frac{H^{(1)}(kr;n)}{H^{(1)}(kR;n)} \int_0^{2\pi} u(R,\phi) e^{\mathbf{i}n(\theta-\phi)} d\phi.$$

Using this expression, we introduce the exact Dirichlet-to-Neumann (DtN) mapping as:

$$M_{exact} u(\theta) \equiv \frac{k}{2\pi} \sum_{n=-\infty}^{\infty} \frac{H^{(1)'}(kR;n)}{H^{(1)}(kR;n)} \int_0^{2\pi} u(R,\phi) e^{\mathbf{i}n(\theta-\phi)} d\phi, \tag{7}$$

which relates the Dirichlet data of the solution u on the artificial boundary Γ_R to the Neumann data on the same boundary. If we put $M = M_{exact}$ in (6), the problem (4)-(6) is equivalent to the original problem (1)-(3). The DtN mapping can also be expressed as the function of the elliptic operator D^2 as:

$$M_{exact} = M_{DtN}(D^2) = k \frac{H^{(1)'}(kR;\sqrt{D^2})}{H^{(1)}(kR;\sqrt{D^2})}, \quad D \equiv -\mathbf{i}\partial/\partial\theta. \tag{8}$$

1.2 Radiation Boundary Conditions

There have been many studies related to the analytical as well as numerical approximations of the DtN mapping. Among them, Engquist and Majda

[1977], Engquist and Majda [1979] introduced a series of non-local approximate radiation boundary condition such as:

$$M_1(D^2) = \frac{\mathbf{i}}{R}\sqrt{k^2R^2 - D^2},$$
$$M_2(D^2) = M_1(D^2) - \frac{1}{2R}\frac{k^2R^2}{(k^2R^2 - D^2)}$$

and so forth. Some local approximate radiation boundary conditions are well used and they are given as

$$M_{1,1}(D^2) = \mathbf{i}k,$$
$$M_{2,1}(D^2) = \mathbf{i}k - \frac{1}{2R}.$$

Those are derived directly from the Sommerfeld radiation condition. Feng [1983] introduced a series of local type operators such as

$$F_3(D^2) = \mathbf{i}k - \frac{1}{2R} + \frac{\mathbf{i}}{8kR^2} - \frac{\mathbf{i}}{2kR^2}D^2,$$
$$F_4(D^2) = \mathbf{i}k - \frac{1}{2R} + \frac{\mathbf{i}}{8kR^2} + \frac{1}{8k^2R^3} - \left(\frac{\mathbf{i}}{2kR^2} + \frac{1}{2k^2R^3}\right)D^2.$$

Bayliss and Turkel [1980] also introduced in a systematic way a hierarchy of local operators:

$$L_n = \prod_{j=1}^{n}\left(\frac{\partial}{\partial r} - \mathbf{i}k + \frac{4j-3}{2r}\right), n \geq 1.$$

On the other hand, related to the finite element method, Kako and Kano [1999] proposed a non-local approximation by a bounded operator as a higher order correction:

$$M_{LK}(D^2) = \mathbf{i}k - \frac{3}{2R} + \frac{1}{R}\left[1 + \frac{1}{2\mathbf{i}kR}\left(\frac{1}{4} - D^2\right)\right]^{-1}.$$

According to our numerical experiments, the exact DtN operator is the best one when it is combined with the appropriate discrete approximation. In the next subsection, we will briefly review the recent results of Nasir et al. [2003] based on a mixed method approximation.

1.3 Finite Element Approximation

To formulate the finite element method for the Helmholtz problem, we introduce a function spaces $V \equiv H^1(\Omega_R)$. Then the weak formulation of the problem is to find $u \in V$ such that

$$a(u,v) - \langle u,v\rangle_M = (g,v)_{\partial\Omega} \qquad \forall v \in V \tag{9}$$

with

$$a(u,v) = \int_{\Omega_R} \left(\frac{\partial u}{\partial r}\frac{\partial \bar{v}}{\partial r} + \frac{1}{r^2}\frac{\partial u}{\partial \theta}\frac{\partial \bar{v}}{\partial \theta} - k^2 u\bar{v} \right) r dr d\theta,$$
$$\langle u,v\rangle_M = \int_0^{2\pi} (Mu)\bar{v}\ R d\theta, \qquad (f,g)_{\partial\Omega} = \int_{\partial\Omega} f\bar{g} d\sigma,$$

where M is one of the operators appeared in the previous section. Let us introduce a finite dimensional subspace V_h of V. Then the finite element approximation is to find $u_h \in V_h$ such that

$$a(u_h, v_h) - \langle u_h, v_h\rangle_M = (g, v_h)_{\partial\Omega}, \qquad \forall v_h \in V_h. \tag{10}$$

In the following, we will introduce the fictitious domain method combined with a fast direct method. For this purpose, we firstly treat a special problem with annulus region.

1.4 Fast Direct Method

In case that Ω_R is an annulus region, we can make a separation of variables with respect to the radial and angular coordinates, and by dividing the intervals into n_r subintervals in radial direction and into n_θ in angular direction, the finite element method gives a linear system:

$$\mathbf{BU} = \mathbf{F} \tag{11}$$

with a separable matrix $\mathbf{B} = (b_{IJ})$, a given vector $\mathbf{f} = (f_I)$ and a solution vector $\mathbf{u} = (u_J)$ where $b_{IJ} = a(\Phi_J, \Phi_I) - \langle \Phi_J, \Phi_I\rangle_M$ and $f_I = (g, \Phi_I)_{\partial\Omega}$. The matrix $\mathbf{B}$ is given by a tensor product form:

$$\mathbf{B} = \mathbf{R}_2 \otimes \mathbf{T}_1 + \mathbf{R}_1 \otimes \mathbf{T}_2 - k^2 \mathbf{R}_1 \otimes \mathbf{T}_1 - \mathbf{e}_{n_r}^{n_r} \mathbf{e}_{n_r}^{n_r T} \otimes \mathbf{M}$$

with a tri-diagonal matrices $\mathbf{R}_i \in C^{n_r \times n_r}$ $(i = 1, 2)$ and circulant matrices $\mathbf{T}_i$ $(i = 1, 2)$ and $\mathbf{M} \in C^{n_\theta \times n_\theta}$. The matrix $\mathbf{M}$ corresponds to the radiation boundary condition and $\mathbf{e}_j^n$ denotes the usual jth canonical basis vector of R^n. Explicit forms for the matrices for $\mathbf{R}_i, \mathbf{T}_i$ and $\mathbf{M}$ can be found, for example, in Ernst [1996].

To solve the system (11), a fast direct solution method based on separation of variables can be used by diagonalizing the circulant matrices. This leads to

$$(\mathbf{I}_{n_r} \otimes \mathbf{Q}^H)(\mathbf{R}_2 \otimes \mathbf{\Lambda}_1 + \mathbf{R}_1 \otimes \mathbf{\Lambda}_2 - k^2 \mathbf{R}_1 \otimes \mathbf{\Lambda}_1$$
$$- \mathbf{e}_{n_r}^{n_r} \mathbf{e}_{n_r}^{n_r T} \otimes \mathbf{\Lambda}_M)(\mathbf{I}_{n_r} \otimes \mathbf{Q})\mathbf{u} = \mathbf{f},$$

where $\mathbf{\Lambda}_i, i = 1, 2$ and $\mathbf{\Lambda}_M$ are diagonal matrices consisting of eigenvalues of the corresponding circulant matrices and $\mathbf{Q}$ is the Fourier matrix with